

The Role of CaMK1D in Alzheimer's Disease

by

Paige Grant

A thesis submitted in partial fulfillment of the requirements for the degree of

Master of Science

Department of Biochemistry

University of Alberta

© Paige Grant, 2022

Abstract

Alzheimer's Disease (AD) is an insidious, progressive neurodegenerative disease responsible for the majority of dementia cases worldwide. Despite extensive research and clinical trials, there are currently no approved treatments that alter the progression of the disease. Treating classic molecular targets of AD, amyloid-beta ($A\beta$) and tau, have not been successful in clinical trials. Further exploration of the disease pathways and of new targets are needed to find effective disease-altering treatments for AD. Here, the role of calcium/calmodulin-dependent protein kinase type 1D (CaMK1D) in AD is examined. While CaMK1D has been implicated in AD in numerous genetic studies, little research has been done at the protein level. In this thesis, mouse primary neuron cultures treated with $A\beta$ oligomers are used as model system for AD, and specific inhibitors for CaMK1D are used to suppress CaMK1D activity in these cultures. These specific inhibitors are characterized kinetically by surface plasmon resonance, and found to have nanomolar level dissociation constants. Western blotting is used to examine $A\beta$ -induced changes in CaMK1D, tau, and Cyclic AMP responsive element binding protein 1 (CREB), a CaMK1D substrate, and cell viability assays are used to examine cell death in culture. The cleavage and phosphorylation state of CaMK1D was unchanged. CaMK1D specific inhibitors were found to ablate $A\beta$ -induced changes to CREB and tau phosphorylation, but did not protect the cells from $A\beta$ -induced toxicity. Aberrant CaMK1D activity is shown to be a potential contributor to AD, but inhibition of this activity is insufficient to protect neurons from death.

Preface

This thesis is an original work by Paige Grant. The research project, of which this thesis is a part, received research ethics approval from the University of Alberta Animal Care and Use Committee: Health Sciences 1, titled “Interrelationships between amyloid beta peptides, the insulin-like growth factor-II/mannose-6-phosphate receptor and central cholinergic neurons: functional and structural implication in Alzheimer’s disease pathology.”, AUP00000271, February 1, 2018. Data and analysis from sections 3.1.3 and 3.5 were submitted to the special issue “New Advances in the Development of Kinase Inhibitors” from the journal *Molecules*.

A problem is a chance for you to do your best.

– Duke Ellington

Acknowledgements

The work presented in this thesis would not have been possible without the help and support of many people. First, I would like to thank my supervisor, Dr. Michael Overduin, for your support and guidance throughout my graduate program. Thank you to my supervisory committee members, Dr. Sue-Ann Mok and Dr. Satyabrata Kar for your feedback and openness. Thanks also go to Dr. Kar for welcoming me into your lab, and providing me with the equipment needed to produce and upkeep my primary cultures. To Dr. Catharine Trieber and Dr. Jitendra Kumar, thank you for lending your advice whenever I needed it. Thank you to Dr. Geetika Phukan for teaching me how to create primary neuron cultures, and to Dr. Qi Wu for help with troubleshooting cell culture problems. Thank you to Dr. Fedor Berditchevski for providing phosphorylation site specific CaMK1D antibodies, and to Dr. Sam Butterworth for providing CaMK1D specific inhibitors. Thank you to undergraduate researcher Trixie Rae Adra for your technical support in this work. To Cameron Smithers, thank you for your support, encouragement, commiseration, and friendship over the years. Thank you as well to past and present Overduin lab members for the talks and laughs.

Thank you to the Alberta Prion Research Institute and the Alzheimer Society of Alberta and Northwest Territories, and the Canadian Institutes of Health Research for providing funding support to this work.

To all my friends and family, thank you for your love and support. Lastly, special thanks go to Arta. You stood by me through the good and bad, and your unwavering belief in me bolstered me every day. Thank you.

Contents

List of Tables	viii
List of Figures	ix
List of Abbreviations	x
1 Introduction	1
1.1 Alzheimer's Disease	1
1.1.1 Brief history of AD	1
1.1.2 Diagnosis of AD	2
1.2 What causes sporadic AD?	3
1.2.1 Risk factors	4
1.2.2 Amyloid cascade hypothesis	4
1.2.3 Tau hypothesis	10
1.2.4 Calcium hypothesis	12
1.2.5 Synergy between hypotheses	16
1.3 Ca ²⁺ /CaM dependant kinases in AD	17
1.3.1 CaMKII	17
1.3.2 CaMKK2	18
1.3.3 CaMKIV	18
1.4 CaMK1D	19
1.4.1 AD relevance	19
1.4.2 Relevance to other diseases	21
1.4.3 CaMK1D inhibitors	23
1.5 Thesis objectives and hypotheses	25
2 Materials and Methods	27
2.1 Protein expression and purification	27
2.1.1 DNA constructs	27
2.1.2 Transformations	27
2.1.3 Expression of CaMK1D	28
2.1.4 Purification of CaMK1D	28
2.2 Binding kinetics of CaMK1D inhibitors	29
2.2.1 Biotinylation of AviTagged TM CaMK1D	29
2.2.2 Surface plasmon resonance (SPR)	29
2.3 Mouse primary cortical neuron cell culture	31
2.3.1 Coating plates	31
2.3.2 Dissection	31
2.3.3 Cell culture preparation	31
2.3.4 Treatment with CaMK1D inhibitors and/or A β ₁₋₄₂	32
2.4 Assaying mouse primary cortical neurons	33

2.4.1	MTT assays	33
2.4.2	LDH assays	33
2.4.3	Western blot and mass spectrometry sample preparation .	34
2.4.4	Western blotting	35
2.4.5	Mass spectrometric analysis	35
3	Results	38
3.1	Analysis of CaMK1D inhibitors	38
3.1.1	Purification of CaMK1D	38
3.1.2	CaMK1D inhibitor binding kinetics	38
3.1.3	Neurotoxicity of CaMK1D inhibitors	43
3.2	Neurotoxicity of A β ₁₋₄₂ oligomers	43
3.3	Phosphorylation and cleavage of CaMK1D	46
3.3.1	Cleavage state of CaMK1D	46
3.3.2	Phosphorylation state of CaMK1D	46
3.4	Activity of CaMK1D	48
3.4.1	Changes to CREB phosphorylation with CaMK1D inhibitor treatment	48
3.5	Effect of CaMK1D inhibitors on the progression of AD-like pathology in cell culture	49
3.5.1	Effect of CaMK1D inhibitors on tau phosphorylation . . .	49
3.5.2	Effect of CaMK1D inhibitors on A β ₁₋₄₂ oligomers neurotoxicity	51
4	Discussion	54
4.1	Properties of CaMK1D inhibitors	54
4.1.1	CaMK1D inhibitors have nanomolar level K _D values . . .	54
4.1.2	CaMK1D inhibitors are non-neurotoxic up to 1 μ M concentrations	55
4.2	CaMK1D is neither hyperphosphorylated nor cleaved in A β ₁₋₄₂ -treated mouse primary neurons	57
4.3	Inhibitors for CaMK1D ablate A β ₁₋₄₂ -induced changes to CREB phosphorylation	60
4.4	CaMK1D inhibitors reduce tau phosphorylation, but not neuron death, in A β ₁₋₄₂ treated cell cultures	61
5	Conclusions and Future Directions	64
5.1	Conclusions	64
5.2	Future Directions	65
	References	67

List of Tables

1.1	AD Risk Factors.	5
2.1	Antibodies Used.	36
3.1	Summary of CaMK1D Inhibitor Binding Kinetics by SPR.	41
4.1	Summary of CaMK1D Inhibitor Properties.	57

List of Figures

1.1	Amyloidogenic and Non-Amyloidogenic APP Processing.	7
1.2	Full length tau domain organization.	10
1.3	Pathological tau regulation in AD.	11
1.4	Calcium homeostasis disturbances in AD.	14
1.5	Structure and domains of CaMK1D.	20
1.6	CaMK1D protein and mRNA level alterations in AD.	22
1.7	Structures and binding of CaMK1D inhibitors.	24
3.1	Purification of Avi-Tagged TM CaMK1D for SPR.	39
3.2	Immobilization of CaMK1D to streptavidin chip.	40
3.3	Compound binding to CaMK1D by SPR.	42
3.4	Effect of varying concentrations of CaMK1D inhibitors on primary neurons	44
3.5	Effect of varying concentrations of A β ₁₋₄₂ on the viability of primary neurons	45
3.6	Lack of evidence for CaMK1D fragments.	47
3.7	Relative abundance of phosphorylated CaMK1D in mouse primary neuronal cell cultures.	47
3.8	Relative abundance of phosphorylated CREB in mouse primary neuronal cell cultures	49
3.9	Relative abundance of phosphorylated tau in mouse primary neuronal cell cultures	50
3.10	Effect of varying concentrations of CaMK1D inhibitors on the viability of primary neurons treated with A β ₁₋₄₂ oligomers	53
4.1	Comparison of the structures of CS640 and CS861.	56
4.2	Model of CaMK1D's involvement in AD.	63

List of Abbreviations

Materials and Reagents

DMSO	Dimethyl Sulfoxide
DNA	Deoxyribonucleic Acid
DTT	Dithiothreitol
ddH ₂ O	Double Distilled Water (Milli-Q®)
ECL	Electrochemiluminescence
EDTA	Ethylenediaminetetraacetic acid
FBS	Fetal Bovine Serum
HBSS	Hank's Balanced Salt Solution
HEPES	N-2-hydroxyethylpiperazine-N-ethanesulfonic acid
HFIP	Hexafluoroisopropanol
IPTG	Isopropyl β-d-1-thiogalactopyranoside
Kan	Kanamycin
LB	Luria-Bertani broth
MTT	3-(4,5-dimethylthiazol-2-yl)-2,5-diphenyltetrazolium bromide
NiNTA	Nickel-nitrilotriacetic acid
PBS	Phosphate Buffered Saline
PDL	Poly-D-Lysine Solution
PVDF	Polyvinylidene Fluoride
RIPA	Radio-Immunoprecipitation Assay buffer
SDS	Sodium Dodecyl Sulphate
SDS-PAGE	Sodium Dodecyl Sulphate–Polyacrylamide Gel Electrophoresis
SOC	Super Optimal Broth with Catabolite Repression media
TBST	Tris Buffered Saline with Tween20

Proteins

Aβ	Amyloid-β
ADAM10	A Disintegrin and Metalloproteinase domain-containing protein 10
AICD	Amyloid Intracellular Domain
AMPA	α-amino-3-hydroxy-5-methyl-4-isoxazolepropionic acid
AMPK	AMP-activated Protein Kinase
ApoE	Apolipoprotein E

APP	Amyloid Precursor Protein
BACE1	Beta-site Amyloid Precursor Protein Cleaving Enzyme 1
BDNF	Brain-derived neurotrophic factor
BirA	<i>E. coli</i> Biotin Ligase
CaM	Calmodulin
CaMK1D	Calcium/Calmodulin-dependent Protein Kinase type 1D
CaMKII	Calcium/Calmodulin-dependent Protein Kinase type II
CaMKIV	Calcium/Calmodulin-dependent Protein Kinase type IV
CaMKK2	Calcium/Calmodulin-dependent Protein Kinase Kinase type 2
CaN	Calcineurin
CDK5	Cyclin-dependent Protein Kinase-5
CK	Casein Kinase
cKLiK	CaMKI-like Kinase
CREB	Cyclic AMP Responsive Element Binding protein 1
CRTC2	CREB-Regulated Transcription Coactivator 2
DYRK	Dual Specificity Tyrosine-phosphorylation-regulated Kinases
GAPDH	Glyceraldehyde 3-phosphate Dehydrogenase
GSK3	Glycogen Synthase Kinase-3
HER2	Human Epidermal Growth Factor Receptor-2
LDH	Lactate Dehydrogenase
TEV	Tobacco Etch Virus protease
HRP	Horse Radish Peroxidase
MAPK	Mitogen Activated Protein Kinase
MARK	Microtubule Affinity-Regulating Kinases
NMDA	N-methyl-D-aspartate
PDPK	Proline-Directed Protein Kinases
PhK	Phosphorylase Kinase
PKA	cAMP-dependent Protein Kinase
PKB	Protein Kinase B
PKC	Protein Kinase C
PKN	Protein Kinase N
PP1	Protein Phosphatase 1
PP2A	Protein Phosphatase 2A
PP2B	Protein Phosphatase 2B
PP5	Protein pPhosphatase 5
PSEN	Presenilin protein
PTEN	Phosphatase and Tensin homolog
sAPP α	Amyloid Precursor Protein soluble ectodomain α
sAPP β	Amyloid Precursor Protein soluble ectodomain β
TORC2	Target of Rapamycin Complex 2
TRPC	Transient Receptor Potential Cation Channels
TTBK	Tau-tubulin Kinases
VGCC	Voltage-gated Calcium Channels
VHL	von Hippel–Lindau protein

Miscellaneous

AD	Alzheimer's Disease
AID	Autoinhibitory Domain
BALB/c	Bagg Albino
CV	Column Volume
HCD	Higher-energy C-trap Dissociation
K_D	Dissociation Constant
k_{off}	Ligand off-rate
k_{on}	Ligand on-rate
LTD	Long-term Depression
LTP	Long-term Potentiation
MCI	Mild Cognitive Impairment
NFT	Neurofibrillary Tangle
NIA-AA	National Institute on Aging-Alzheimer's Association
PCR	Polymerase Chain Reaction
PHF	Paired Helical Filament
PROTAC	Proteolysis Targeting Chimeras
SNP	Single Nucleotide Polymorphisms
TNBC	Triple Negative Breast Cancer

Chapter 1

Introduction

1.1 Alzheimer's Disease

Alzheimer's Disease (AD) is a progressive neurodegenerative condition which is the most common cause of dementia worldwide[1]. It is characterized by a slow decline in cognition including memory loss, which is the most widely recognized AD symptom, as well as poor judgement, difficulty communicating, and personality and behavioural changes[2]. At the molecular level, AD is characterized most notably by neurofibrillary tangles (NFTs) and neuritic plaques, made up of aggregated tau and amyloid- β ($A\beta$), respectively[3]. There are currently no effective treatments that successfully alter the progression of AD. There are two general types of AD: sporadic and genetic. The genetic forms of the disease typically onset prior to the age of 65, and are caused by mutations in amyloid precursor protein (APP), or one of the presenilin proteins (PSEN), which are involved in the processing of APP[4] (Section 1.2.2). Most AD cases are sporadic, and generally onset after the age of 65. While the precise cause of sporadic AD is not known, the main risk factor is advanced age. This thesis is focused on sporadic AD.

1.1.1 Brief history of AD

AD was first described by Alois Alzheimer in 1907, when he reported his findings regarding his patient Auguste D[5, 6]. In this initial report, Alzheimer noted that motor disturbances were not observed, rather the disease was characterized by cognitive decline. The disease was described to begin with feelings of jealousy,

followed by progressive memory impairment, and ending with severe apathy. The patient often repeated the phrase “Ich hab mich verloren”, which translates to “I have lost myself”. The post-mortem studies of the brain revealed marked brain atrophy, fibrils within the neurons, and “a deposition of a peculiar substance in the cerebral cortex” in the extracellular space, later known to be A β plaques[5, 6]. Similar observations are still used today in the diagnosis of AD clinically and post mortem.

1.1.2 Diagnosis of AD

In clinics today, the criteria for diagnosis of AD essentially consists of diagnosing dementia, and then ruling out other possible causes of the dementia[2]. The 2011 revision of the National Institute on Aging-Alzheimer’s Association (NIA-AA) diagnostic guidelines[2] outlines the parameters required for an AD diagnosis, which are generally adopted in Canada[7]. These diagnostic criteria are briefly summarized here. A diagnosis of dementia of any cause is characterized by cognitive changes that (a) interfere with the ability to conduct activities of daily life, (b) show a decline from previous cognitive level, (c) cannot be explained by delirium or other psychiatric disorders, (d) are observed through both detailed history and objective mental status examination or neuropsychological testing, and (e) demonstrates impairment in at least two cognitive domains. Cognitive domains that can be affected include impaired acquisition and memory of new information, impaired reasoning and judgement, impaired visuospatial abilities, impaired language functions, and behavioural and personality changes. A patient that fits these criteria can be diagnosed with dementia, and the cause of the dementia can be further investigated[2]. A diagnosis of probable AD requires that the patient (a) meets the criteria for a diagnosis of dementia, (b) experiences insidious onset over months or years, (c) has a clear history of worsening cognition, (d) initial presentation either follows amnesic onset (learning and memory problems) or non-amnesic onset (language, visuospatial, or executive function deficits), (e) there are no indications of cerebrovascular disease, dementia with Lewy bodies, frontotemporal dementia, primary progressive aphasia, or any other diseases or medications that

could interfere with cognition[2]. AD can also coexist with other forms of dementia, which can complicate diagnosis[8, 9]. At this time, biomarkers are not included in the clinical criteria for probable AD diagnosis, though they can be used when available, at the discretion of the physician. While these criteria are helpful in informing clinical decision making during the patient's life, they only provide a probable diagnosis; they are not definitive.

Post mortem, AD pathology can be assessed. Based on established criteria, AD is highly likely when both A β plaques and NFTs are present in an advanced stage in the neocortex, moderately likely when there are a moderate amount of A β plaques and NFTs in the limbic region, and unlikely when there are very few A β plaques and NFTs[3, 10]. Staging and severity to determine likelihood are based on CERAD[11] or Braak and Braak[12] staging. AD dementia is pathophysiologically proved only when a patient meets the clinical criteria and when pathological indications of AD are present.

1.2 What causes sporadic AD?

While genetic AD is caused by mutations in APP or PSEN, the precise root cause(s) of sporadic AD remain unknown. However, there are many hypotheses regarding the molecular mechanisms behind the disease, and many of these hypotheses have compelling data to support them. Strong cases have been made for viewing A β as the causal agent[13, 14], similarly strong cases have been made for viewing AD as a tauopathy[15]. There is clear data to support calcium homeostasis as a main driver[16, 17], as well as neuroinflammation[18]. Other hypotheses centre around DNA damage[19], autophagy[20] and lysosomal loss of function[21], impaired cell cycle control[22], oxidative stress[23], glucose metabolism[24], and loss of mitochondrial function[25]. While each of these hypotheses have merits, this thesis will focus mainly on the amyloid cascade hypothesis, the tau hypothesis, and the calcium hypothesis. These are three of the most widely studied hypotheses, and aspects of each of these contribute to the hypotheses and objectives of this thesis (Section 1.5).

1.2.1 Risk factors

Above all else, the biggest risk factor for sporadic AD is increasing age. Every 5 years after the age of 65, the prevalence of dementia approximately doubles[26, 27].

Differing alleles of the gene encoding apolipoprotein E (ApoE) can either increase or decrease the risk of sporadic AD. The *ApoE3* allele is the most common, and the risk factors of other alleles are compared to *ApoE3* homozygotes. The *ApoE4* allele is deleterious and the *ApoE2* allele is protective. People that are heterozygous for *ApoE4* are about 2.8 times more likely to receive an AD diagnosis in their lifetime than people homozygous for the *ApoE3* allele, while *ApoE4* homozygotes are 8 times more likely to receive a diagnosis[28]. *ApoE4* also effects the age of onset of AD, with each added *ApoE4* allele decreasing the age of onset. Homozygotes for *ApoE4* have a mean age of onset of 68.4 years, heterozygotes have a mean age of onset of 75.5 years and patients carrying no ApoE4 allele have a mean age of onset of 84.3[28]. Heterozygotes for *ApoE2* have a decreased risk of developing AD by a factor of 4. Homozygotes for *ApoE2* are rare, and thus do not have statistically significant data[29]. The benefit of the *ApoE2* allele and the risk of the *ApoE4* allele lessen with age[29].

While the factors that confer the greatest risk of AD cannot be changed, there are some risk factors for sporadic AD that are modifiable based on an individual's lifestyle, health care, and other factors. Of these factors, physical inactivity, defined by doing neither 20 min of rigorous activity on 3 or more days in a week, nor 30 min of moderate activity on 5 or more days in a week, confers the greatest relative risk at 1.82 times[30]. Other modifiable risk factors include depression, midlife obesity, midlife hypertension, smoking, low educational attainment, and diabetes mellitus[30]. AD risk factors, their definitions, and their relative risks are outlined in Table 1.1.

1.2.2 Amyloid cascade hypothesis

The most well studied hypothesis regarding the root cause of sporadic AD is the amyloid cascade hypothesis. It was formally proposed in 1992 by Hardy and Hig-

Table 1.1: AD Risk Factors.

Alzheimer's disease risk factors, their definitions, and the relative risk of developing AD. Adapted from Norton et al. 2014[30].

Risk Factor	Definition	Relative Risk
<i>ApoE4</i>	Homozygous <i>ApoE4</i> allele	8
	Heterozygous <i>ApoE4</i> allele	2.8
Physical Inactivity	Does neither 20 min of rigorous activity on 3 or more days in a week, nor 30 min of moderate activity on 5 or more days in a week	1.82
Depression	Lifetime presence of a major depressive disorder	1.65
Midlife Hypertension	Presence of hypertension between the ages of 35 years and 64 years	1.61
Midlife Obesity	Body-mass index greater than 30 kg/m ² between the ages of 35 and 64 years	1.60
Smoking	Adult smoker	1.59
Low Educational Attainment	International Standard Classification of Education level of 2 or less (pre-primary, primary, and lower secondary education)	1.59
Diabetes Mellitus	Diagnosed diabetes mellitus between the ages of 20 and 79 years	1.46
<i>ApoE2</i>	Heterozygous <i>ApoE2</i> allele	0.25

gins[13], though other groups had similar ideas around the same time [31–33]. The hypothesis centres on the processing of APP and the behaviours of its cleavage product, A β , as the driving force of AD.

In a non-amyloidogenic process, APP, a single pass integral membrane protein, is first cleaved close to the membrane by an α -secretase, a disintegrin and metalloproteinase domain-containing protein 10 (ADAM10)[34], then it is cleaved on the intracellular side by a γ -secretase. PSENs are the catalytic component of the γ -secretase complex. This produces three benign fragments, the APP soluble ectodomain α (sAPP α), p3, and amyloid precursor protein intracellular domain (AICD)[35, 36] (Figure 1.1). However, in an amyloidogenic process, APP is instead cleaved by a β -secretase, beta-site amyloid precursor protein cleaving enzyme 1 (BACE1)[37], which cleaves APP in a location further from the membrane than the α -secretase, followed by the same γ -secretase cleavage. This produces APP soluble ectodomain β (sAPP β), A β , and AICD[35, 36] (Figure 1.1). The A β fragment, on which this hypothesis centres, can be between 38-43 amino acids in length, depending on precisely where γ -secretase creates the C-terminus of the peptide[38, 39]. These peptides form oligomers and plaques in the extracellular space due to their high propensity for aggregation. The most common isoforms are 40 and 42 amino acids in length, with longer peptides such as A β ₄₂ being more toxic and aggregation prone[40]. While A β plaques and fibrils were long thought to be the toxic form of A β , in the last 20 years, soluble oligomers have been shown to be the toxic species[41–43]. In the simplest terms, the amyloid cascade hypothesis suggests that sporadic AD is caused by a sequence of events resulting directly from the action of these A β peptides, oligomers and/or plaques.

Some strong evidence in favour of the amyloid cascade hypothesis is based on the effects of mutations in APP and its processing proteins in familial AD. These mutations are found both in APP itself and in PSEN1 and PSEN2, the catalytic subunits of γ -secretase. Various disease causing mutations in APP can favour amyloidogenic APP processing, favour the production of longer A β peptides, or directly influence the aggregation kinetics of A β itself. The Swedish variant (KM670/671NL)[44], along with several other APP mutations[4], promotes amyloidogenic

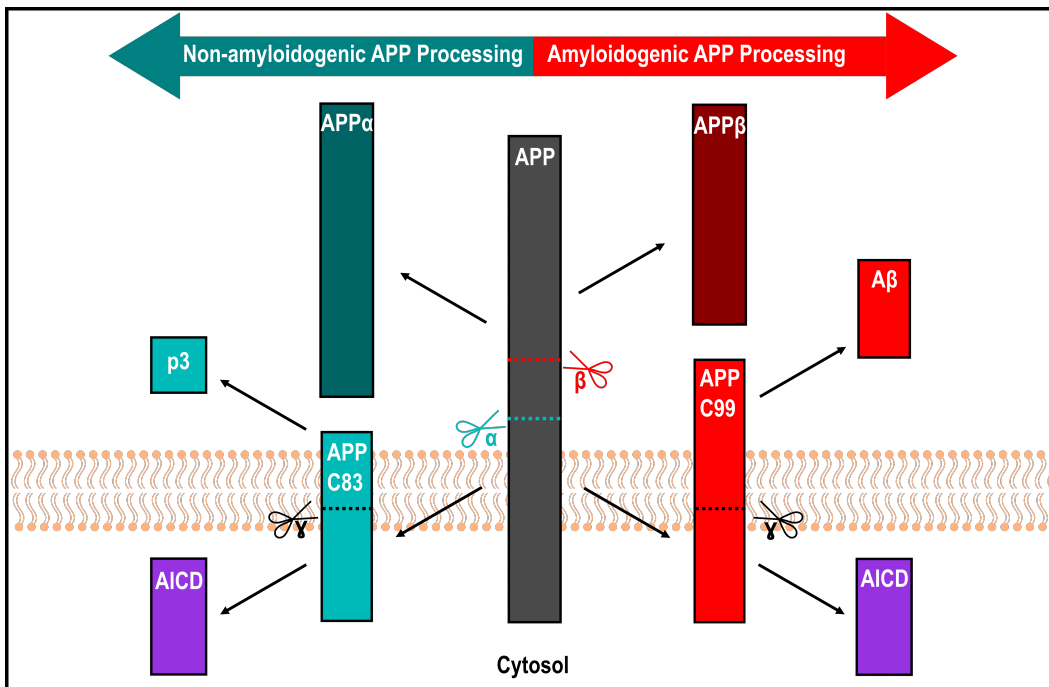


Figure 1.1: **Amyloidogenic and Non-Amyloidogenic APP Processing.**

Fragments produced from non-amyloidogenic processing are shown in teal, fragments from amyloidogenic processing are shown in red, and fragments common to both processes are shown in purple.

Adapted from Lucía Chávez-Gutiérrez and Maria Szaruga 2020[4].

processing of APP by favouring cleavage of APP by β -secretase over α -secretase. Some deleterious mutations favour the production of longer, more toxic and aggregation prone A β peptides by influencing the precise site of cleavage by γ -secretase[4]. Note that these mutations are not present in the resulting A β peptide, and thus do not directly influence the aggregation kinetics of the peptide; these mutations simply favour the production of longer, more toxic A β fragments. However, there are other mutations, such as the Arctic E693G variant, that are within the A β peptide and result in more aggregation prone peptides, regardless of length[45]. Based on this evidence alone, it is clear that APP, APP processing, and A β peptides make an important contribution to familial AD.

There have been almost 300 familial AD linked mutations identified in PSEN1, and about 10 in PSEN2. Each of these mutant proteins retains protease activity, but may be impaired. The γ -secretase complex has both ϵ -endopeptidase activity, with which it makes the first cut, and processive γ -activity, with which it sequentially shortens the peptide[38, 39]. Most familial AD-linked mutations impair γ -secretase's ϵ -endopeptidase activity to some extent, but, importantly, all of the familial AD linked mutations have impaired processivity[4]. The result of this is a higher proportion of longer, more toxic A β peptides produced, with most of these mutations resulting in increased A β 42/40 ratios. Some of these mutations also influence γ -secretase independent activities of PSEN, but these are inconsistent across mutations. Processing of A β by γ -secretase also makes a clear contribution to genetic forms of AD.

Evidence for the A β hypothesis that is not related to familial AD also exists. First, ApoE variants have differential effects on soluble A β clearance in mice, with ApoE4, the AD risk factor discussed in section 1.2.1, leading to the least A β clearance[46]. Treatment of cultured rat neurons with A β oligomers also leads to an AD-like hyperphosphorylation of tau[47, 48], and injection of A β oligomers into rodent hippocampus decreases synapse density, inhibits long-term potentiation (LTP, a process that promotes strong synaptic connections and synaptic plasticity), and enhances long-term synaptic depression (LTD, a process that reduces efficacy of synaptic connections)[49]. Accumulation of A β also precedes other AD

markers and symptoms[50].

While the evidence in favour of the amyloid cascade hypothesis is plentiful, numerous failures in clinical trials targeting APP processing and A β directly have called its validity into question. As of early 2019, every clinical trial focused on improving clearance of A β or reducing production of A β had failed to show clinical efficacy, despite indications in many cases of improvements in A β load[51]. These have cast significant doubt on the A β hypothesis, with some suggesting abandoning it entirely[52]. Since then, there has been very little success. The only potential success story is Aducanumab, a monoclonal antibody targeting A β oligomers and fibrils, though its efficacy is still unclear. A phase III trial with Aducanumab was halted in March of 2019 due to futility. Later that year, however, it was announced that after further analysis, a subset of patients receiving a sufficient dose of the antibody did show efficacy, and the antibody would be submitted for a New Drug Application with the Food and Drug Administration. This abrupt change in interpretation was certainly unconventional and led to criticism, particularly due to incomplete data reporting and insufficiently explained differences between two Aducanumab trials[53, 54]. Currently, it is unclear whether Aducanumab is a promising candidate to be celebrated, or a drug doomed to fail like the rest.

Based on this evidence, it remains unclear whether the A β hypothesis should be accepted or rejected. Clearly, there is a strong correlation between A β and AD, despite cases where A β accumulation exists, but the patient shows no clinical signs of the disease[3]. However, thus far, no drug that prevents A β production or increases clearance has shown clinical efficacy. It is possible that drugs tested thus far have not shown high enough specificity for the responsible species of A β , that they have been given too late in the progression of AD, or that dosage and endpoints in clinical trials need adjustment. It is also possible that an increase in A β in the AD brain is an epiphenomenon, or that reduction of A β load is necessary, but not sufficient, to slow the progression of AD. While it is possible that other targets may be impacted by similar challenges, regardless, it is prudent to approach the disease from different directions, rather than focusing only on clearance or preventing production of A β .

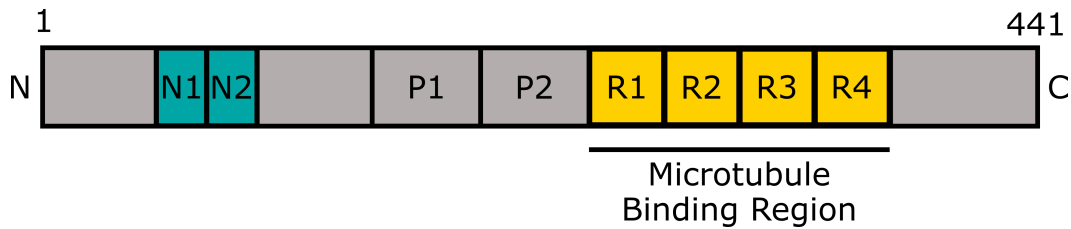


Figure 1.2: **Full length tau domain organization.**

Domain organization of the longest isoform of tau (2N4R). N-terminal inserts are labelled as N, proline rich regions are labelled as P, and tubulin binding domains are labelled as R. Adapted from Shamma et al. 2015 [56].

1.2.3 Tau hypothesis

Another well studied hypothesis regarding the root cause of AD is the tau hypothesis. In a healthy neuron, tau is a microtubule-associated-protein. It binds to tubulin and stabilizes microtubules, particularly in the axon. Microtubules are involved in multiple cell processes such as cell division, cell morphogenesis, and intracellular trafficking, and are a vital component of a healthy neuron. There are six possible isoforms of tau, resulting from alternative splicing. These can include either 3 or 4 tubulin binding domains (3R or 4R), and either 0, 1, or 2 inserts in the N-terminal region (0N, 1N, or 2N). Each isoform also includes two proline rich regions which are N-terminal to the tubulin binding repeats, an N-terminal region, and a C-terminal region (Figure 1.2). In healthy neurons, almost all tau is bound to microtubules, with very little being freely cytosolic or localized elsewhere[55].

In AD, tau undergoes abnormal post-translational modifications, the most well studied of these being hyperphosphorylation. There are about 80 potential phosphorylation sites in the 2N4R isoform of tau, most of which are located in the proline rich and C-terminal domains[55]. When tau is hyperphosphorylated, it cannot bind tubulin. It falls off of microtubules, destabilizing them, preventing elongation and promoting their disassembly[57]. This loss of function alone is damaging for the cell, as microtubule functions are impaired and intracellular transport by kinesin and dyenin are compromised. However, hyperphosphorylated tau also gains a toxic function. In the cytoplasm of neurons, it aggregates into structures such as single straight filaments and paired helical filaments (PHF) which subsequently

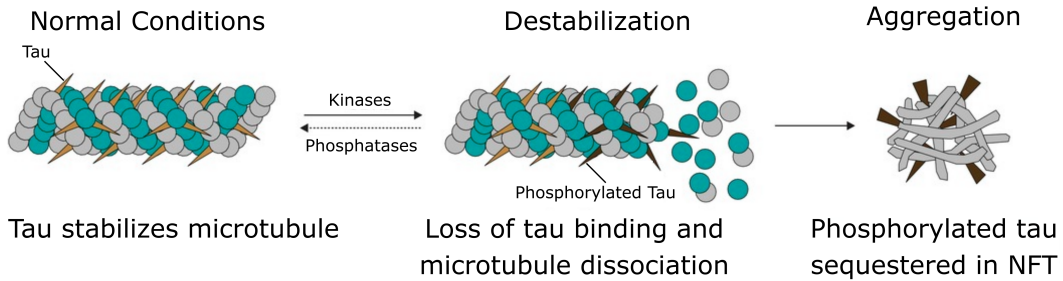


Figure 1.3: **Pathological tau regulation in AD.**

Hyperphosphorylation of tau causes it to dissociate from microtubules, destabilizing them. Tau then forms aggregate structures. Adapted from Bachurin et al. 2017[59].

lead to the formation of NFTs[55]. These structures have also been shown to be able to transfer between cells, potentially recruiting tau from adjacent cells and contributing to the spread of AD pathology through the brain[58]. The tau hypothesis suggests that these tau aggregate structures are responsible for the degeneration of neurons and progression of AD.

There are numerous potential candidates involved in the hyperphosphorylation of tau, including both upregulated kinases and downregulated phosphatases. The kinases fall into two categories: proline-directed protein kinases (PDPK) and non-PDPK. PDPKs include glycogen synthase kinase-3 (GSK3), cyclin-dependent protein kinase-5 (CDK5), and mitogen activated protein kinases (MAPKs) such as JNK, p38 and ERK. Non-PDPKs include tau-tubulin kinases (TTBK), casein kinases (CK), dual specificity tyrosine-phosphorylation-regulated kinases (DYRK), microtubule affinity-regulating kinases (MARK), phosphorylase kinase (PhK), cAMP-dependent protein kinase (PKA), protein kinase B (PKB), protein kinase C (PKC), protein kinase N (PKN), and Calcium/calmodulin-dependent protein kinase type II (CaMKII). A more comprehensive review of these kinases and their individual roles can be found here[60]. The best studied tau kinase is GSK3. GSK3 phosphorylates tau at 29 sites which are found in AD brains, and in animal models has been shown to be involved in tau hyperphosphorylation, which is reversible by lithium, a GSK inhibitor[61]. GSK is implicated in tau mediated neurodegeneration in the hippocampus, and learning impairment[62]. It has also been linked to

memory deficit, inflammatory response, increased production of A β and reduced acetylcholine synthesis [60, 63]. However, despite the wealth of data surrounding GSK's role in AD, the GSK inhibitor Tideglusib failed to meet clinical endpoints in a phase II clinical trial[64]. On the side of phosphatases, protein phosphatase 1 (PP1), protein phosphatase 2A (PP2A), calcineurin (CaN) also known as protein phosphatase 2B (PP2B), protein phosphatase 5 (PP5) and phosphatase and tensin homolog (PTEN) have all been implicated in the dephosphorylation of tau, but PP2A is responsible for over 70 % of total phosphatase activity towards tau [65, 66]. Endogenous inhibitors of PP2A have increased activity in AD brains[67], and, interestingly, GSK3 stimulates phosphorylation of PP2A at Tyr307, a site which inactivates PP2A[68]. Along with several other factors, these lead to reduced PP2A activity by about half in the AD brain[66]. Increased activity of kinases and reduced activity of phosphatases both play a role in the production of hyperphosphorylated tau.

Recently, after multiple failures in targeting A β in AD, tau targeting has become the topic for a great deal of AD clinical research. Drugs have been developed to target various areas of tau pathology, including expression, post-translational modifications, aggregation, microtubule disassembly, and immunotherapy for tau aggregates[65]. While preclinical studies showed promising results, clinical trials completed so far have either failed to meet their endpoints or had unacceptable side effects[69]. These have included tau kinase inhibitors, tau aggregation inhibitors, and microtubule stabilizers. No tau targeting immunotherapies have yet completed phase II clinical trials, with various trials underway[69]. Following failures of A β targeting immunotherapies with similarly promising preclinical results, the results of these trials will be particularly interesting.

Similar to the A β hypothesis, it remains unclear whether tau is the main driver of AD. However, there is clear evidence that it is involved and contributes to AD.

1.2.4 Calcium hypothesis

Calcium ions (Ca²⁺) are important in neurons for neurotransmitter release, synaptic plasticity, gene expression, and many other cellular functions. Concentrations

of Ca^{2+} are tightly controlled by various Ca^{2+} receptors, channels, pumps, antiporters, buffers and sensors, with each having an important role in maintaining Ca^{2+} homeostasis[70]. In a rested state, cytoplasmic Ca^{2+} concentrations are close to 100 nM, while endoplasmic reticulum levels are 100-800 μM , and extracellular levels are 1-2 mM, both much higher than the cytoplasm[71]. Calcium stimulation of the cell, in which cytoplasmic Ca^{2+} levels can rise up to 3 μM , can thus be achieved by both release of Ca^{2+} from intracellular stores, or Ca^{2+} entering from the extracellular space[70]. When entering from the extracellular space, Ca^{2+} is transported via N-methyl-D-aspartate (NMDA) receptors and α -amino-3-hydroxy-5-methyl-4-isoxazolepropionic acid (AMPA) receptors, both of which are activated by glutamate, as well as voltage-gated calcium channels (VGCC), activated by depolarized membrane potentials, and transient receptor potential cation channels (TRPC), activated by phospholipase C[70]. It binds to Ca^{2+} binding proteins, including the important effector of Ca^{2+} function, calmodulin (CaM)[72]. This in turn activates a myriad of CaM dependent proteins, including various Ca^{2+} /CaM dependent protein kinases[72] (Section 1.3) and CaN[73], a Ca^{2+} /CaM dependent protein phosphatase. Each of these CaM activated proteins stimulate their own signalling cascades, leading to many downstream effects. Some of these include neurotransmitter release, membrane excitation, gene transcription, proliferation, and programmed cell death[70].

In AD, regulation of Ca^{2+} levels in the cell are disrupted, and thus, so are many of the downstream effects of Ca^{2+} stimulation[70]. The calcium hypothesis of AD suggests that these disturbances in Ca^{2+} homeostasis are the driving factor of AD[16, 72].

Changes in the NMDA receptors in AD, and in particular, the effect of $\text{A}\beta$ on NMDA receptors in AD have been the subject of significant research. Memantine, a non-competitive NMDA receptor antagonist, is approved as a symptomatic treatment for moderate to severe AD[74, 75]. NMDA receptors have differential effects on neurons based on their degree of activity and localization; synaptic NMDA receptors and activation to a high intracellular Ca^{2+} level promote LTP, while extrasynaptic NMDA receptors and activation to a moderate intracellular Ca^{2+} level

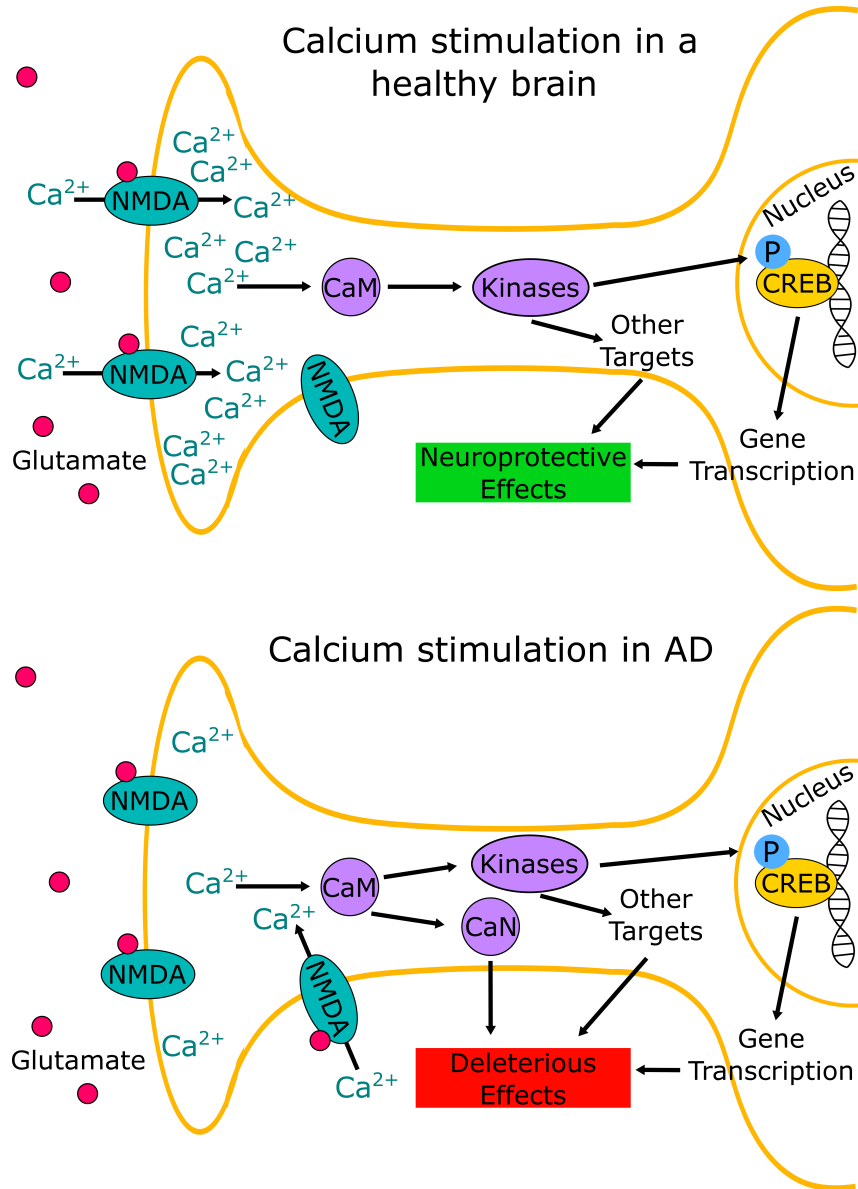


Figure 1.4: **Calcium homeostasis disturbances in AD.**

Calcium homeostasis is altered in AD. In healthy neurons, a stimulation of synaptic NMDA receptors leads to a high level of Ca²⁺ influx. This stimulates CaM, which leads to the stimulation of CaM dependent kinases, which can lead to phosphorylation of CREB and other targets. Overall, this produces a neuroprotective effect. In AD, synaptic NMDA receptors become desensitized to glutamate. Glutamate spills out of the synaptic cleft and activates extrasynaptic NMDA receptors, leading to a moderate, sustained Ca²⁺ influx. This still leads to the activation of CaM and downstream kinases, and potentially the phosphorylation of CREB. It also leads to the activation of CaN. Overall, this sustained, moderate Ca²⁺ stimulation leads to deleterious effects.

promote LTD (Figure 1.4)[76]. While the effect of A β on NMDA receptors is likely complex, in essence A β prevents uptake of glutamate from synapses, elevating synaptic glutamate levels such that synaptic NMDA receptors become desensitized to glutamate, while also spilling glutamate out of the synapse and activating extrasynaptic NMDA receptors[75, 77, 78]. As a result, LTD is promoted over LTP. While there are likely other contributors, NMDA receptors are certainly key proteins involved in the process of causing sustained, moderated increases in Ca²⁺ levels which are deleterious to the cell[75].

CaM is one of the main effectors of Ca²⁺ function, and it is involved in numerous pathways in cells. It is activated by binding Ca²⁺, and itself activates Ca²⁺/CaM dependent proteins. In terms of direct CaM involvement in AD, CaM binding has been shown to increase activity of BACE1 2.5 fold *in vitro*[79], presumably pushing the processing of APP towards the amyloidogenic side. CaM also binds tau in a Ca²⁺ dependent manner, which decreases its microtubule binding[80], but also prevents tau phosphorylation by PKC[81]. CaM is also able to activate CaN (Figure 1.4). When hyperactive, CaN impairs memory formation[82, 83], while CaN inhibitors in AD model mice improve memory formation[84]. Interestingly, CaN has also been shown to dephosphorylate tau at Ser262, Ser369, Thr181, and Thr231, which could be expected to be neuroprotective, though other phosphatases are considered to be more important in this process[85]. Further downstream effects of CaM in AD, particularly Ca²⁺/CaM dependent kinases, will be discussed in section 1.3.

Further downstream in Ca²⁺ dependent signalling pathways, Cyclic AMP responsive element binding protein 1 (CREB), a phosphorylation dependent transcription factor, has also been implicated in AD. CREB is activated by phosphorylation at Ser133 by Ca²⁺ dependent kinases such as calcium/calmodulin-dependent protein kinase type IV (CaMKIV) and calcium/calmodulin-dependent protein kinase type 1D (CaMK1D) (Figure 1.4)[86, 87], and can also be activated by phosphorylation at this site by other kinases that are not Ca²⁺ dependent[88]. This allows CREB to bind DNA and turn on expression of many genes, including the neuroprotective factor brain-derived neurotrophic factor (BDNF)[89]. A few stud-

ies have demonstrated reduced total CREB and phosphorylation of CREB in cell culture models and post-mortem AD brain samples [86, 90–92]. Curiously, there have also been studies that show the opposite. In a human neuroblastoma cell line (SH-SY5Y) expressing a familial AD PSEN1 mutation, and in an AD mouse model (3xTg-AD), CREB was constitutively phosphorylated, with about 3 times higher phosphorylation levels than controls[93]. Another study showed that phosphorylated CREB accumulates in granules in post-mortem AD hippocampus, but was depleted in the nucleus[94]. These differences may be explained by differential effects of Ca^{2+} entry through synaptic vs extrasynaptic NMDA receptors, with the former promoting CREB activation and the latter promoting CREB inactivation[75, 89, 95]. In both cases, CREB activation is clearly altered in AD.

1.2.5 Synergy between hypotheses

Of course, none of these hypotheses exist in a vacuum, and there are clear connections and synergy between them. To highlight a few examples, $\text{A}\beta$ oligomers have been shown to result in increased tau phosphorylation in culture[48, 96, 97]. Conversely, secreted tau results in increased $\text{A}\beta$ levels in culture[98]. $\text{A}\beta$ also stimulates increased Ca^{2+} concentrations in neurons[99], but conversely CaM regulates APP and BACE1 [79, 85]. CaMKII, which is dependent on Ca^{2+} for its activity, is a tau kinase[100], but pathogenic tau depletes nuclear Ca^{2+} in neurons [101]. There is evidence for each major AD player to cause the AD type alterations to the other major AD players.

Altogether, there are clear connections between the $\text{A}\beta$ hypothesis, the tau hypothesis, and the calcium hypothesis of AD. It remains unclear whether one of these is the main driver of AD, whether two or all three of them work synergistically to cause the disease, or whether other factors are necessary to drive the disease. However, it is certainly clear that each of these processes have a role to play, whether as upstream drivers of the disease or as deleterious downstream effects.

1.3 Ca²⁺/CaM dependant kinases in AD

As alluded to in section 1.2.4, there are several Ca²⁺/CaM dependent kinases that have been implicated in AD, which is predictable given the disturbance in Ca²⁺ homeostasis in AD. These kinases are inactive until bound by Ca²⁺ and Ca²⁺ activated CaM.

1.3.1 CaMKII

The calcium-dependent kinase that has been the most extensively studied in relation to AD is CaMKII. Comprised of 12 subunits, it can be homomeric or heteromeric, including α , β , γ and/or δ subunits, with α and β CaMKII being the most abundant[102]. α CaMKII is involved in synaptic plasticity and memory formation[103], while β CaMKII, which binds F-actin, is mainly structural[104, 105]. CaMKII is activated by Ca²⁺/CaM binding, but can be decoupled from Ca²⁺/CaM activation by autophosphorylation at Thr286. When Thr286 is phosphorylated, CaMKII remains active independent of Ca²⁺/CaM binding. Phosphorylation at this site is important for spatial memory formation and LTP[102, 106]. Activated CaMKII also leads to a signalling cascade that results in the phosphorylation of the transcription factor CREB[107].

In AD, while expression of CaMKII seems to remain unchanged, the subcellular localization of CaMKII and of CaMKII phosphorylated at Thr286 is altered[108]. For both total CaMKII and phosphorylated CaMKII, localization is reduced in dendrites and synapses, but increased in the cell body[109]. Reduction of phosphorylated CaMKII at Thr286 in dendrites is associated with cognitive dysfunction in AD and mild cognitive impairment (MCI) patients[108]. Spatial training of APP_{Swe} mice increased CaMKII autophosphorylation and improved spatial memory formation, suggesting CaMKII autophosphorylation is involved in AD memory formation and synaptic plasticity deficits[110]. CaMKII is also a tau kinase at several sites that are found to be phosphorylated in PHFs, and likely contributes to tau hyperphosphorylation and formation of NFTs[100]. Selectively inhibiting CaMKII in primary cortical neurons can reduce A β induced tau phosphorylation and cas-

pase activity[111]. Overall, CaMKII has a wealth of evidence as a contributor to AD.

1.3.2 CaMKK2

Calcium/calmodulin-dependent protein kinase kinase type 2 (CaMKK2), a serine/threonine protein kinase, has also been implicated in AD[112]. It has several isoforms produced by alternative splicing, and phosphorylates various proteins, including AMP-activated protein kinase (AMPK) and CaMK1D[112, 113].

In AD models, A β oligomers activate AMPK in a CaMKK2 dependent manner. Both CaMKK2 and AMPK are required for the synaptotoxic effects of A β oligomers *in vitro*, and for dendritic spine loss in mouse models of AD[112]. AMPK is able to phosphorylate tau on Ser262, altering tau binding to microtubules and contributing to its hyperphosphorylation[114]. Both dendritic spine loss and tau phosphorylation at Ser262 can be rescued by microRNA interference in CaMKK2 expression[115]. Aberrant AMPK activation by CaMKK2 also leads to dysregulation of mitophagy, causing mitochondrial loss in dendritic spines and dendritic spine loss through downstream AMPK pathways[116]. Through pathways that are not well understood, CaMKK2 may also deregulate iron homeostasis in AD through aberrant transferrin phosphorylation[117].

1.3.3 CaMKIV

Another Ca²⁺/CaM dependent kinase that has been implicated in AD is CaMKIV, though its role in the disease is not well studied. CaMKIV is another serine/threonine protein kinase, which is involved in various signalling pathways, including directly phosphorylating CREB on Ser133[107]. It is involved in memory formation and consolidation, and reduced expression of CaMKIV is associated with normal aging memory loss[118]. Phosphorylation by a CaMKK at Thr200 activates the protein[119]. In AD models, CaMKIV shows reduced nuclear translocation, no change in expression levels, and increased phosphorylation[86, 120]. It has been suggested that this may lead to constitutive CREB phosphorylation in AD models[93].

1.4 CaMK1D

The CaMK1D protein is a member of the CaMKI family of Ca^{2+} /CaM dependent protein kinases, which consists of four isoforms (α , β , γ , δ) from separate genes. CaMK1D itself also has four reported splice variants, the first being aptly named CaMK1D, the second CaMKI-like kinase (cKLiK), and the last two, both of which are inactive forms of the kinase, have been recently reported as CaMK1D-b and CaMK1D-d[121]. While cKLiK is expressed only in polymorphonuclear leukocytes[122], the CaMK1D splice variant is the most ubiquitously expressed variant, with expression in liver, spleen, thymus, testes, ovaries, colon, and brain[113], with the brain exhibiting the highest expression[87].

CaMK1D's domain structure is similar to that of other CaMK proteins, including CaMKK2, CaMKII and CaMKIV (Section 1.3), consisting of a kinase domain, a CaM binding domain (CBD), and an autoinhibitory domain (AID) that overlaps the CBD (Figure 1.5). CaMK1D activity is Ca^{2+} /CaM dependent, and mostly CaMKK dependent, with low basal activity without CaMKK activation[113, 121]. In an inactive state, CaMK1D's AID sits along the surface of the active site, blocking the enzymatic activity. Binding of CaM results in exposure of the active site as the AID relocates. This both allows a CaMKK to access the activation loop, phosphorylating and activating it at Thr180[113], as well as allows the active site to access substrates. One such substrate is CREB, a phosphorylation dependent transcription factor (Section 1.2.4). CaMK1D can phosphorylate CREB at Ser133, activating it[87]. As such, CaMK1D has a role in CREB-dependent gene transcription. It has been additionally shown to promote basal dendritic growth of hippocampal neurons[123].

1.4.1 AD relevance

Given CaMK1D's association with AD-implicated proteins, including CaM and CREB, as well as its dependence on Ca^{2+} for activity, it is not surprising that CaMK1D has been implicated in AD. Numerous studies have examined the gene that codes for CaMK1D, aptly named *CaMK1D*, in AD. A genomic convergence

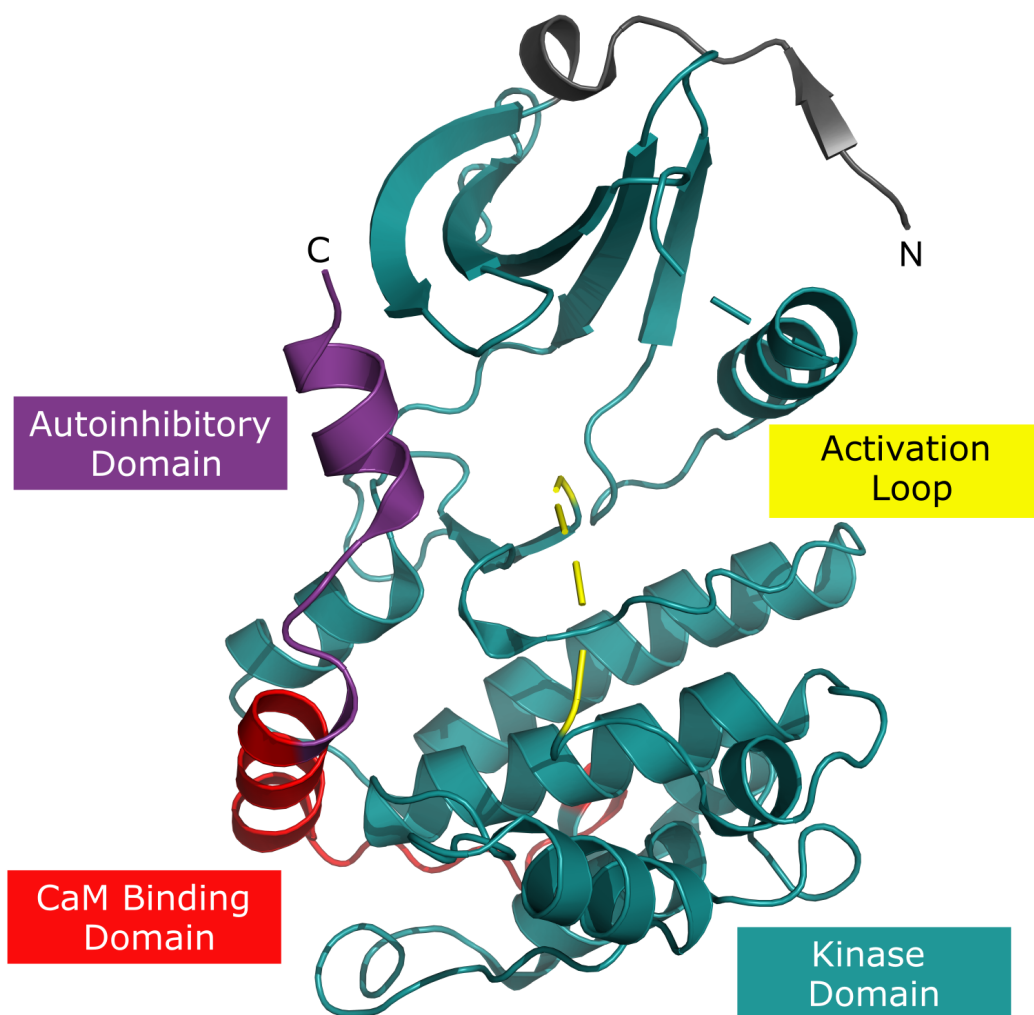


Figure 1.5: **Structure and domains of CaMK1D.**

Crystal structure of CaMK1D (PMID: 2JC6). The AID is shown in purple, CBD is shown in red, activation loop is shown in yellow, and the conserved kinase domain is shown in teal. Any part of the protein that does not belong to these categories is shown in grey. Dashed lines indicate areas of incomplete electron density in the crystal structure. The beta strand shown near the N-terminus is isolated because in this structure CaMK1D crystallized as a dimer, with which this strand interacts. The dimer is excluded from view. The small molecule included in this structure (PDB code: QPP) is also excluded from view.

study first showed an association between single nucleotide polymorphisms (SNP) in *CaMK1D* and AD[124], and subsequently, a genome-wide association study also identified *CaMK1D* as having SNPs associated with established AD SNPs[125]. Two peer-reviewed studies on hydroxymethylation of *CaMK1D* have also shown associations with AD patients post-mortem[126, 127]. One of these identified *CaMK1D* as one of only four genes with hydroxymethylation that was associated with clinical AD, as well as with both A β plaques and NFTs in post-mortem brain samples[126]. Another study examined the hydroxymethylation of DNA in blood samples from control and AD patients, and found alterations to *CaMK1D*. These authors suggested *CaMK1D* hydroxymethylation as a diagnostic marker for AD[128]. Despite the genetic and epigenetic evidence for CaMK1D's involvement in AD, little research has been performed on CaMK1D in AD at the mRNA or protein level. In one study, CaMK1D mRNA levels in AD post-mortem basal forebrain samples were found to be downregulated by 75 % compared to normal aged controls (Figure 1.6 A). Similarly, protein levels in AD basal forebrain were found to be downregulated by 63 % compared to normal aged controls (Figure 1.6 B-C). Interestingly, western blots for CaMK1D in post-mortem basal forebrain samples revealed unidentified bands at smaller sizes than full length CaMK1D, with one band about 15 kDa in size being unique to AD samples (Figure 1.6 B, D). The authors suggest that these may be CaMK1D fragments resulting from proteolysis, though this idea was not validated experimentally[129]. Additionally, CaMK1D is activated by CaMKK2, and activates CREB, both of which have established links to AD[86, 112]. Overall, it is clear that CaMK1D is a potential player in AD, though it remains under studied.

1.4.2 Relevance to other diseases

While the role of CaMK1D in AD will be the focus of this work, CaMK1D also has links to type II diabetes and triple negative breast cancer (TNBC)[130, 131]. In type II diabetes, cells do not respond normally to insulin stimulation, and energy usage and glucose metabolism are altered. Several genome-wide association studies have shown SNPs in *CaMK1D* to be associated with increased prevalence of type

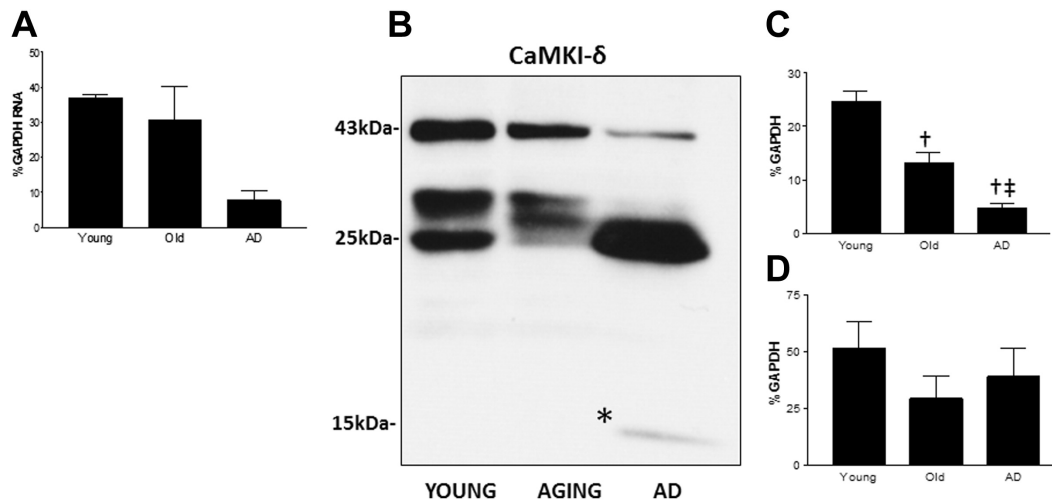


Figure 1.6: CaMK1D protein and mRNA level alterations in AD.

A) CaMK1D mRNA levels in basal forebrain cholinergic neurons from young, aged and AD brains. In AD, mRNA levels are reduced by 75 % compared to normal aged controls. B) Representative western blot for CaMK1D from basal forebrain of young, aged and AD individuals. The full length CaMK1D was observed at 43 kDa, and several unidentified bands were observed between about 25 and 35 kDa. An unidentified light band at about 15 kDa was occasionally seen, exclusively in AD samples (indicated by *). C) Quantification of full length CaMK1D normalized with glyceraldehyde 3-phosphate dehydrogenase (GAPDH) in young, aged and AD basal forebrain. CaMK1D levels were reduced by 63 % in AD brains compared to normal aged controls. D) Quantification of unidentified bands from 25 to 35 kDa normalized with GAPDH in young, aged and AD basal forebrain. No significant differences were observed. Figure from Riascos et al. 2014[129].

II diabetes[132–135], and siRNA knockdown of CaMK1D was associated with loss of nuclear translocation of the established diabetes target CREB-regulated transcription coactivator 2 (CRTC2) (previously named target of rapamycin complex 2 (TORC2)), as well as decreased gluconeogenesis and increased glycogen deposition[136]. Recently, CaMK1D inhibitors were shown to restore insulin sensitivity in diet-induced obese mice[137].

TNBC is a subtype of breast cancer with negative expression of estrogen, progesterone, and human epidermal growth factor receptor-2 (HER2), which is highly invasive, displays poor prognosis, and currently has no targeted therapies[138]. CaMK1D is overexpressed in 80 % of these tumours[130, 139], and engineered overexpression of CaMK1D in non-tumorigenic breast epithelial cells led to increased cell proliferation, and molecular and phenotypic similarities to an epithelial-mesenchymal transition[130]. Mouse models overexpressing CaMK1D also suggest involvement in proliferation and impairment of apoptosis[140].

1.4.3 CaMK1D inhibitors

Various inhibitors have been developed for CaMK1D, intended for *in vitro* and *in vivo* studies on diabetes and triple-negative breast cancer, and two of these compounds were able to improve insulin sensitivity in diet-induced obese mice [137]. Three inhibitors will be used here; inhibitor CS587, inhibitor CS640 and inhibitor CS861 (Figure 1.7). Each of these are competitive inhibitors that engage CaMK1D in the ATP binding pocket. Both inhibitors CS587 and CS640 have IC_{50} values for CaMK1D in the nanomolar range for at both the enzymatic and cellular levels[137]. Both also show a strong selectivity for CaMK1D over related kinases, including over CaMKIV. However, due to highly conserved active sites within the CaMKI family, these compounds have limited selectivity for CaMK1D over other CaMKI isoforms[137]. Inhibitor CS861 is a proteolysis targeting chimeras (PROTAC) molecule, existing as a conjugate of inhibitor CS640 and a von Hippel–Lindau protein (VHL) recruiting ligand with an amide attachment[141]. PROTACs function by recruiting VHL, part of the E3 ubiquitin ligase complex, to the protein of interest, causing the protein to be polyubiquitinated and targeted for

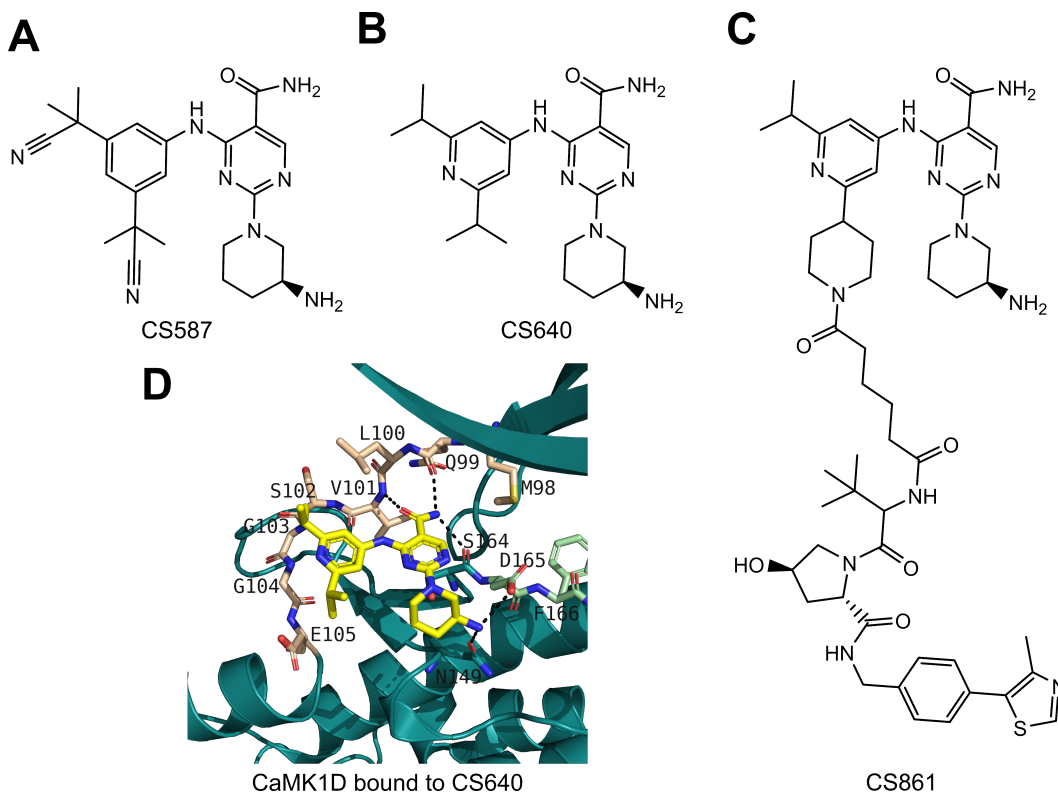


Figure 1.7: **Structures and binding of CaMK1D inhibitors.**

Structures of A) CS587, B) CS640, C) CS861 and D) CS640 bound to CaMK1D in the ATP binding pocket. The P-loop has been made transparent for better visibility. Panel D is adapted from Fromont et al. 2020[137].

degradation by the proteasome, rather than simply inhibiting the protein[141, 142]. Because PROTACs depend on only a transient, reversible association with the target protein, rather than the prolonged association needed for a competitive inhibitor, they are less likely to result in drug resistance compared to traditional small molecule inhibitors. For the same reason, PROTACs are also less sensitive to changes in target protein expression levels and substrate concentrations[142]. As CS861 has been developed more recently, its IC_{50} values and selectivity have not yet been published, but as the CaMK1D binding portion is nearly identical to CS640, it can reasonably be expected to behave similarly at the enzymatic level.

1.5 Thesis objectives and hypotheses

While inhibitors for CaMK1D have been used in mice, and IC_{50} values have been published[137], some critical information about these inhibitors is missing from the literature. First, the binding affinity and kinetics have not yet been established. These are important for determining dosage in cell culture and animal studies. Additionally, the effect of these inhibitors on the brain, and neurons in particular, has not been studied. If these inhibitors are to be useful in AD studies, they should be non-toxic to neurons at effective concentrations informed by the IC_{50} values and binding kinetic data. Given the high expression of CaMK1D in the brain, and its importance for dendritic growth of hippocampal neurons, inhibition of CaMK1D in neurons may be detrimental. These properties of CaMK1D inhibitors will need to be established before moving forward with studies using them.

While there is clear evidence that CaMK1D is altered in AD, there is little research regarding the nature of this involvement. The potential for CaMK1D cleavage [129] is particularly interesting, given that CaMK1D is regulated by CaM binding and removing the AID from blocking the active site and activation loop. If CaMK1D was cleaved such that these two domains were removed, CaMK1D regulation would become decoupled from Ca^{2+} /CaM activation. Additionally, the activation loop would be perpetually accessible to a CaMKK, and, understanding that CaMKK2 is itself deregulated in AD, this could lead to hyperphosphorylation and hyperactivity of CaMK1D.

Hyperactive CaMK1D could have detrimental effects in the brain. Aberrant phosphorylation of CREB[93] could disrupt homeostasis of CREB-dependent gene transcription. Since CREB is involved in the transcription of many genes, the cascade of downstream effects would be numerous. Additionally, CaMK1D likely has undiscovered substrates, as altered CREB activity alone cannot explain the role of CaMK1D in TNBC and diabetes. Aberrant phosphorylation of these may also be detrimental. Hyperactive CaMK1D may phosphorylate proteins that it generally would not interact with in a healthy cell. Being constantly "on" gives CaMK1D more opportunity to act aberrantly. CaMK1D inhibitors may be able to prevent or

reverse these effects by reducing CaMK1D activity to a normal level.

The objectives of this thesis are:

1. Determine characteristics of CaMK1D inhibitors including binding kinetics to CaMK1D and toxicity to neuronal cells.
2. Further the understanding of the state and role of CaMK1D in an AD model, including its cleavage and phosphorylation state, and the impact of CaMK1D inhibitors.

My hypotheses are:

1. Inhibitors for CaMK1D can be used in cell culture experiments at effective concentrations without toxicity.
2. CaMK1D becomes cleaved and/or hyperphosphorylated which causes it to be deregulated in AD.
3. Inhibitors for CaMK1D can control the progression of AD-like pathology in cell culture.

Chapter 2

Materials and Methods

All chemicals were research grade and obtained from MilliporeSigma or Thermo Fisher Scientific unless otherwise indicated.

2.1 Protein expression and purification

2.1.1 DNA constructs

DNA constructs used here were prepared previously[143]. CaMK1D constructs from amino acids 1-333 were expressed in a pNIC28-Bsa4 vector, which uses a T7 promoter. This vector added an N-terminal His₆ tag to the expressed protein for use in purification, as well as a tobacco etch virus protease (TEV) cleavage site between the His₆ tag and CaMK1D to allow for production of protein without a His₆ tag. One construct also included an AviTagTM N-terminal to CaMK1D, and C-terminal to the TEV cleavage site, to allow for biotinylation of the protein and subsequent use in SPR studies.

2.1.2 Transformations

Rosetta 2 (DE3) competent cells were first thawed on ice, after which 2 μ L of DNA was added and the cells were gently mixed by flicking the tube. This was left on ice for 30 min. The cells were then heat-shocked in a 42°C dry bath for 30 s, and returned to ice for 2 min. After this time on ice, 250 μ L of super optimal broth with catabolite repression media (SOC) media warmed to 37°C was added to the cells, and these were grown at 37°C with 180 rpm shaking for 1 h. These were

then spread on Luria-Bertani broth (LB) plates with 50 µg/mL kanamycin (Kan) and incubated overnight at 37°C, after which colonies could be seen.

2.1.3 Expression of CaMK1D

A small scraping of cells from a glycerol stock or from a plate was added to 20 mL of LB media containing 50 µg/mL Kan, and grown overnight at 37°C with shaking at 180 rpm. If cells were taken from a plate, a glycerol stock was made from 500 µL of overnight culture and 500 µL 80% glycerol, and this was stored at -80°C. Overnight cultures were transferred into 1 L of LB containing 50 µg/mL Kan, and grown at 37°C to an optical density of approximately 0.6. At this point, 1 mM isopropyl β-d-1-thiogalactopyranoside (IPTG) was added to induce expression and the temperature was reduced to 18°C. Cultures were incubated with shaking at 180 rpm overnight. After expression, cultures were centrifuged for 20 min at 10 000 ×g and the supernatant was discarded. Cell pellets were weighed and stored at -80°C.

2.1.4 Purification of CaMK1D

This protocol is performed entirely at 4°C or on ice. This purification protocol is adapted from previous work[143]. Half of a cOmpleteTM EDTA-free protease inhibitor cocktail tablet from Roche was added to 25 mL of CaMK1D binding buffer (50 mM HEPES, 500 mM NaCl, 20 mM imidazole, 2 mM calcium chloride, 0.05 % Tween20, 0.5 mM TCEP, pH 7.5), and this was added to a 4-6 g cell pellet and re-suspended. The cell suspension was homogenized using a Dounce homogenizer. Keeping the cell suspension on ice, the cells were sonicated four times with a probe sonicator for 45 s, with a 1 s on/off pulse, at 75% amplitude with a 1 min rest between each round of sonication. This was then centrifuged at 90 000 ×g for 45 min. In the meantime, 5 mL of nickel-nitrilotriacetic acid (NiNTA) resin was equilibrated with about 10 column volumes (CV) of CaMK1D binding buffer by gravity flow. After centrifugation, the supernatant was added to the NiNTA resin, and incubated with agitation for 1.5 h. The flow-through was collected, and the column was washed with 20-30 CV of CaMK1D binding buffer. Washing was

stopped when 10 μ L of wash no longer turned 10 μ L of BioRad protein assay solution blue, indicating that little to no protein was leaving the column. The resin was then incubated with agitation for 15 min with 5 mL of CaMK1D elution buffer (CaMK1D binding buffer with 500 mM imidazole), and CaMK1D was eluted. If removal of the His6 tag was required, 1 mL of TEV protease was added to the eluate. CaMK1D protein was then dialysed against CaMK1D buffer (CaMK1D binding buffer without imidazole) overnight. If TEV protease had been added, a reverse NiNTA column was required following dialysis. To run this column, the CaMK1D, TEV, and free His6 tag mixture was added to 5 mL of NiNTA resin and incubated for approximately 1 h. The CaMK1D without a His6 tag was then collected in the flow through, while the TEV, free His6 tag and Ni-NTA-binding contaminants remained bound to the column. The concentration of purified CaMK1D was determined by BioRad protein assay. Purified CaMK1D was either stored at 4°C and used within 5 days for binding kinetic studies, or 20 % glycerol was added and the protein was flash frozen in liquid nitrogen and stored at -80°C for antibody optimization western blots.

2.2 Binding kinetics of CaMK1D inhibitors

2.2.1 Biotinylation of AviTaggedTM CaMK1D

As *E. coli* biotin ligase (BirA), an enzyme capable of covalently attaching biotin to an AviTagTM, is inactive in high salt conditions, AviTaggedTM CaMK1D was concentrated so that salt from the CaMK1D buffer in the end reaction would be no higher than 100 mM. The reaction mixture contained 50 mM bicine buffer pH 8.3, 10 mM ATP, 10 mM MgOAc, 50 μ M d-biotin, 40 μ M CaMK1D and 10 μ g of BirA enzyme. The reaction mixture was incubated overnight at 4°C, and the next day the buffer was exchanged back to CaMK1D buffer using a 10 kDa centrifuge filter.

2.2.2 Surface plasmon resonance (SPR)

All solutions were filtered (0.22 μ m) and degassed before use, and the flow rate was set to 30 μ L/min on a Biacore T200 system. Channels 1 and 2 of a strepta-

vidin chip from Cytiva were primed with three consecutive 60 s injections of 1 M NaCl in 50 mM sodium hydroxide. Approximately 40 μ M biotinylated CaMK1D in CaMK1D buffer was then injected onto channel 2 of the chip for 10 s, followed by a 30 s wash with CaMK1D buffer, then another 10 s CaMK1D injection. SPR running buffer (50 mM HEPES, 150 mM NaCl, 2 mM calcium chloride, 0.05 % Tween20, 0.001 % sodium azide, 0.5 mM TCEP, pH 7.5) was run through the chip at an increased flow rate of 90 μ L/min for a further 140 s to equilibrate the chip and check for loss of response. Channel 1 was left blank.

Compound binding kinetics were then tested using association/dissociation experiments. All compounds were dissolved in SPR running buffer, with residual 0.002 % dimethyl sulfoxide (DMSO) from the compound stock solution. For compound CS587, the flow rate used was 30 μ L/min, contact time for each concentration of compound was 30 s, and dissociation time was 240 s. After running these experiments, the contact and dissociation time were determined to be too short, so for both CS640 and CS861 contact time was increased to 300 s, and dissociation time was increased to 600 s. Between each injection of compound, the channels were washed with 0.35 M EDTA for 30 s, followed by a 180 s stabilization period before moving on to the next concentration of compound.

For analysis, the response from channel 1 was subtracted from the response from channel 2. Binding kinetics were first analysed in the Biacore T200 analysis software, using a 1:1 binding model. This model analyzes the entire dataset holistically, calculating one value of k_{on} , k_{off} , and K_{D} for the entire dataset. These values were compared to values obtained from an association then dissociation non-linear regression in GraphPad Prism; this model analyses each binding curve individually. Each concentration and replicate are fit separately, and individual k_{on} and k_{off} are obtained. This individual analysis method enabled informed elimination of poor quality and outlier binding curves from the analysis, for example in the case of too high or too low concentrations of compound. For the remaining curves, k_{on} and k_{off} values were averaged, and the average k_{off} was divided by the average k_{on} to calculate the average K_{D} .

2.3 Mouse primary cortical neuron cell culture

2.3.1 Coating plates

A 10×poly-d-lysine (PDL) solution was prepared by adding 25 mL of phosphate buffered saline (PBS) (Gibco PBS, pH 7.4) to 5 mg of PDL. This was sonicated in an ultrasonic bath for 10 min. For use in coating plates, this solution was diluted ten-fold in PBS. The day before dissection, 1 mL of 1×PDL was added to each well in 6 well plates, or 50 µL per well in 96 well plates, and these were incubated at 37°C and 5 % CO₂ overnight. The morning of the dissection, the PDL was aspirated, plates were rinsed twice with autoclaved Milli-Q® water (ddH₂O), and plates were dried in a biosafety cabinet.

2.3.2 Dissection

Dissections were performed as described previously[48, 96]. A pregnant female Bagg albino (BALB/c) mouse was euthanised on day 18 of her pregnancy, and the fetal mice were excised from the uterus. Inside a biosafety cabinet, the fetal mice were decapitated, and heads were placed in a 60 mm culture dish containing approximately 20 mL of warm Hank's balanced salt solution (HBSS) (Gibco HBSS with added 0.6 mM L-glutamine, 30 units/mL penicillin, 30 µg/mL streptomycin, 1 mM sodium pyruvate, and 10 mM HEPES pH 8). Brains were excised from the skulls using Fisherbrand™ Tapered Ultrafine Tip Forceps and a Feather #10 scalpel, and these were placed in a second culture dish containing 20 mL warm HBSS. The remaining dissection steps were completed under a light microscope. Meninges were removed from the brains, and the cortices were dissected out using the same forceps. Cortices were placed in a 15 mL conical tube containing 5 mL of warm HBSS.

2.3.3 Cell culture preparation

Primary cell cultures were prepared as described previously[48, 96]. The cortices were allowed to settle to the bottom of the tube, and the HBSS was aspirated. Immediately, 5 mL of room temperature Gibco TrypLE Express was added to the

tissue, and the conical tube was placed in a 37°C water bath for 15 min. Following this incubation, the TrypLE Express was aspirated, and 10 mL of warm HBSS+ (HBSS with added 10 % fetal bovine serum (FBS)) was added to the tissue. A 10 mL pipette was used to triturate the tissue until it appeared homogeneous. A 40 µm cell strainer was wet with 3 mL of warm HBSS+, and the cell suspension was filtered through this to ensure only single cells remained. The conical tube and 10 mL pipette were rinsed with 2 mL of warm HBSS+ and this was added through the strainer as well. The single cell suspension was centrifuged at 500 ×g for 5 min. The HBSS+ was aspirated, and 10 mL of warm neurobasal media #1 (Gibco Neurobasal media with added 0.6 mM L-glutamine, 30 units/mL penicillin, 30 µg/mL streptomycin, 1 mM sodium pyruvate, 10 mM HEPES pH 8, 1 % FBS, and 1×B-27 supplement) was used to resuspend the cells. A 10 µL aliquot of cells was mixed with 10 µL of BioRad Trypan Blue 0.4 %, and cells were counted using a BioRad TC20™ automated cell counter. Once counted, cells were plated on PDL coated 6 well plates (2 mL of media/well, 1.5×10^6 cells/well) or 96 well plates (100 µL of media/well, 5×10^4 cells/well), and kept in a 37°C and 5 % CO₂ incubator. After 24 h, the cell media was changed to warm neurobasal media #2 (neurobasal media #1 without FBS). After another 96 h (4 d) the media was changed again to warm neurobasal media #3 (neurobasal media #2 without B-27 supplement and with 1×N2 supplement). Following 24 h in this media, cells were visually inspected under a microscope, and were used in experiments if they had the expected morphology.

2.3.4 Treatment with CaMK1D inhibitors and/or Aβ₁₋₄₂

Aβ₁₋₄₂ peptides were obtained from rPeptide, and oligomerized as described previously[144]. These were monomerized by dissolving in hexafluoroisopropanol (HFIP) followed by sonication in an ultrasonic bath for 1 min. The solution was separated into 10 aliquots in low protein binding polymerase chain reaction (PCR) tubes, and the HFIP was evaporated in a fume hood to create 0.1 mg monomer films. These were stored at -20°C until use. When ready for use, an aliquot was sonicated in a bath sonicator with 5 µL of DMSO to dissolve the film. Following this, 20 µL of autoclaved ddH₂O was added, and the Aβ₁₋₄₂ was left to oligomer-

ize at 4°C for 16 h. CaMK1D inhibitors were stored in 10-50 mM stock solutions dissolved in 100 % DMSO, and were diluted in ddH₂O to 100X the intended media concentration for use in cell culture experiments. DMSO was added to lower concentrations of inhibitor in order to match the residual DMSO from the highest concentration used. Oligomerized A β ₁₋₄₂ and/or CaMK1D inhibitors were diluted in neurobasal media #3 and added to the cell cultures in the desired concentrations. Total DMSO concentration in cell culture remained below

2.4 Assaying mouse primary cortical neurons

2.4.1 MTT assays

Primary cells were treated with the desired A β ₁₋₄₂ oligomers and/or CaMK1D inhibitors. The low MTT signal control was treated with 10 μ L of 100 % DMSO, and the maximum MTT signal control was treated with only 0.4 % DMSO, to match the amount of DMSO in experimental wells. All treatments lasted 24 h. Following these treatments, the media was aspirated, and was replaced with 5 mg/mL MTT reagent from Invitrogen diluted ten times in neurobasal media #3. The cells were incubated in a 37°C and 5 % CO₂ incubator for 4-6 h, after which the MTT media was carefully aspirated, leaving the purple formazan crystals, and replaced with 50 μ L of DMSO in each well. Plates were shaken gently for 5 min, and absorbance was read at 630 and 570 nm. Absorbance readings at 630 nm were subtracted from those at 570 nm, to control for any small changes in turbidity between wells. MTT assays depend on the metabolic activity of the cell, and therefore measure cell viability. The viability was then calculated using the following formula:

$$\text{Viability(\%)} = \frac{\text{Experimental MTT Signal}}{\text{Maximum MTT Signal}} \times 100 \quad (2.1)$$

2.4.2 LDH assays

Primary cells were treated with the desired with A β ₁₋₄₂ oligomers and/or CaMK1D inhibitors for 24 h, and lactate dehydrogenase (LDH) assays were performed using Promega's CytoTox 96® Non-Radioactive Cytotoxicity Assay. The low LDH release control cells were treated with only 0.4 % DMSO, to match the amount of

DMSO in experimental wells, while the maximum LDH release control was treated with 10 μ L of 10 \times Lysis Solution. After these treatments, 50 μ L of media were transferred to a fresh 96 well plate, and 50 μ L of CytoTox 96[®] Reagent was added. The plate was protected from light, and incubated at room temperature for 30 min to 1 h. After this, 50 μ L of stop solution was added, and absorbance was read at 630 and 490 nm. Absorbance readings at 630 nm were subtracted from those at 490 nm, to control for any small changes in turbidity between wells. LDH assays measure release of LDH from the cell, which occurs when the cell membrane ruptures and the cellular contents leak into the media. These assays therefore measure cytotoxicity, rather than viability. The cytotoxicity was calculated using the following formula:

$$\text{Cytotoxicity(\%)} = \frac{\text{Experimental LDH Release} - \text{Low LDH Release}}{\text{Maximum LDH Release} - \text{Low LDH Release}} \times 100 \quad (2.2)$$

2.4.3 Western blot and mass spectrometry sample preparation

After treatment with A β ₁₋₄₂ and/or CaMK1D inhibitors, 6 well plates containing primary neurons were placed on ice, and media was aspirated. Plates were rinsed twice with ice cold PBS, and cells were removed by scraping each well in 500 μ L ice cold PBS. Cell suspensions for each plate were pooled, transferred to 5 mL conical tubes and centrifuged for 5 min at 500 \times g. The PBS supernatant was then aspirated. Cell pellets were flash frozen in liquid nitrogen, and stored at -80°C . Once needed, cells were thawed on ice, and 1.5 μ L of RIPA+ buffer (150 mM NaCl, 1 % Triton X-100, 0.5 % deoxycholate, 0.1 % sodium dodecyl sulphate (SDS), 50 mM TrisHCl pH 8.0, 25 mM NaF, 20 mM sodium pyrophosphate, 10 mM sodium orthovanadate and 1:50 Sigma-Aldrich protease inhibitor cocktail P8340) per mg of cell mass was added to the cell pellet. Cells were lysed by ten freeze thaw cycles, freezing in a dry ice and ethanol bath and thawing in a room temperature water bath. Lysates were centrifuged at 21 000 \times g for 1 h, and the supernatant was transferred to a new microcentrifuge tube. Protein concentration of the supernatant was determined by BioRad protein assay, and the results of this assay were used to ensure even loading of gels used for western blots. BioRad 2 \times Laemmli sample buffer with added 5 mM

dithiothreitol (DTT) was combined with equal volume of supernatant, and samples were heated at 95°C for 10 min. If SDS–Polyacrylamide Gel Electrophoresis (SDS-PAGE) gels were to be run at a later date, these samples were stored at –20°C.

2.4.4 Western blotting

Gradient SDS-PAGE gels (4–20 %) from Bio-Rad were loaded so that the amount of protein in each lane was equal. Gels were run at 225 V for 27 min in SDS running buffer (25 mM Tris, 192 mM glycine, and 0.1 % SDS), and wet transferred to a methanol-activated polyvinylidene fluoride (PVDF) membrane at 80 V for 1 h in transfer buffer (25 mM Tris, 192 mM glycine). Membranes were incubated with agitation in blocking buffer (2 % fish skin gelatin, 25 mM NaF, 20 mM sodium pyrophosphate, 10 mM sodium orthovanadate, 20 mM Tris pH 7.5 and 150 mM NaCl) for 1-4 h. Primary antibodies were diluted in blocking solution, and incubated with the membranes at 4°C. Dilutions and time of incubation for each antibody is outlined in Table 2.1. Membranes were washed once for 10 min, followed by three times for 5 min in Tris buffered saline with Tween20 (TBST) (20 mM Tris pH 7.5, 150 mM NaCl and 0.1 % Tween20). Secondary antibodies were diluted 1:3000 in blocking buffer and incubated with membranes for 2-4 h at room temperature. Membranes underwent one 10 min wash, followed by three 5 min washes in TBST, before incubating with electrochemiluminescence (ECL) substrate for 5 min. Membranes were imaged using a Licor Odyssey® Fc imaging system and quantified by densitometry using ImageJ.

2.4.5 Mass spectrometric analysis

SDS-PAGE gels were loaded with 40-60 µg protein total, and run at 225 V for 27 min in SDS running buffer. Gels were stained with coomassie stain (0.25 g/L Coomassie R250, 25 % isopropanol, and 10 % acetic acid), and destained with destaining solution (20 % methanol and 10 % acetic acid). The gel lane was cut into small slices by size, using the molecular weight markers as a guide. The remaining steps of the in-gel digestion and protein identification analysis were performed by the Alberta Proteomics and Mass Spectrometry Facility. Each gel section was subjected

Table 2.1: Antibodies Used.

A summary of the features and usage of antibodies used for western blotting.

Antibody Name	Type	Species	Antigen/ Epitope	Obtained From	Dilution	Incubation Time
Anti-Mouse	HRP-linked 2°	Goat	Mouse IgG	Bio-Rad	1:3000	2-4 h
Anti-Rabbit	HRP-linked 2°	Goat	Rabbit IgG	Cell Signalling Technologies	1:3000	2-4 h
AT270	1°	Mouse	Tau/ pT181	Thermo Fisher Scientific	1:250	16 h
β -Actin	1°	Mouse	β -Actin/ 2-16	Sigma-Aldrich	1:1000	16 h
CaMK1D	1°	Rabbit	CaMK1D/ 350-C	Abcam	1:5000	2 h+
CREB	1°	Rabbit	CREB/ 250-350	Abcam	1:1000	4 h+
GAPDH	1°	Mouse	GAPDH	Sigma-Aldrich	1:5000	16 h
pCaMK1D	1°	Rabbit	CaMK1D/ pS179 & pT180	Gift from Fedor Berdichevski	1:250	16 h
pCREB	1°	Rabbit	CREB/ pS133	Abcam	1:250	16 h
Tg5	1°	Mouse	Tau	Gift from Peter Davies	1:500	16 h

to an in-gel trypsin digestion, and tryptic peptides were resolved and ionized by nano flow HPLC on an EASY-nLC 1000 system using an EASY-SprayTM HPLC Column (75 μm diameter, 15 cm length, 100 \AA pore size, 3 μm particle size). This was coupled to a Q Exactive Orbitrap mass spectrometer in data-dependent acquisition mode using external mass calibration, recording high-accuracy and high resolution Orbitrap spectra with a resolution of 35000 and a mass to charge ratio of 300-1700. The twelve most intense multiply charged ions were sequentially fragmented using higher-energy C-trap dissociation (HCD), and their Orbitrap spectra were recorded at a resolution of 17 500. Precursors selected for dissociation were then dynamically excluded for 30 s. Data was processed in Proteome Discoverer 1.4 (Thermo Fisher Scientific), and database searching was performed using SEQUEST (Thermo Fisher Scientific).

Chapter 3

Results

3.1 Analysis of CaMK1D inhibitors

3.1.1 Purification of CaMK1D

In order to be used in binding studies, AviTaggedTM CaMK1D first had to be purified and biotinylated (Figure 3.1). After the NiNTA column, CaMK1D, observed at the expected size around 40 kDa, was at about 60 % purity. Full TEV cleavage was achieved, as observed by the downward shift of the CaMK1D band following this step. The 27 kDa band in the TEV cleavage sample is TEV itself, which is removed by the reverse Ni-NTA column. After the reverse NiNTA column, AviTaggedTM CaMK1D was purified to >80 % purity, measured by densitometry. This was an acceptable purity for SPR using a streptavidin chip, as the biotinylation procedure used here should only add biotin to the AviTagTM, and the streptavidin chip should only bind biotinylated proteins.

3.1.2 CaMK1D inhibitor binding kinetics

Binding kinetics of CaMK1D inhibitors were explored in order to determine a reasonable range of inhibitor concentrations to use in cell culture experiments. Biotinylated CaMK1D was immobilized to the level of about 4000 RU (Figure 3.2). CaMK1D inhibitor compounds CS587, CS640 and CS861 were each tested for binding kinetics (Table 3.1). Tests with compound CS587 resulted in the lowest quality data, likely due to the shorter contact times and dissociation times used. Because of the quality of the data, the Biacore T200 analysis software could not be used

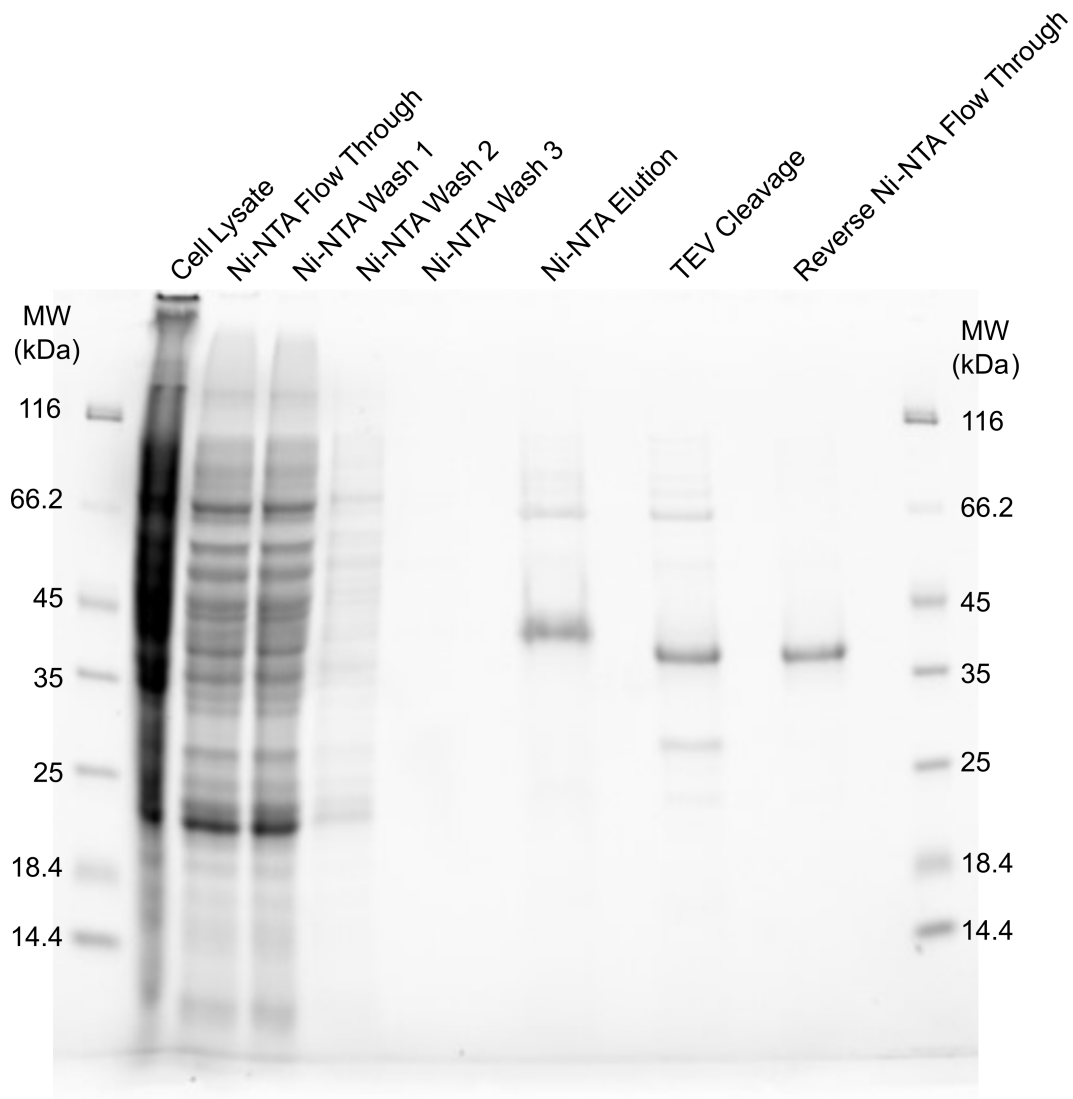


Figure 3.1: **Purification of Avi-TaggedTM CaMK1D for SPR.**
 SDS-PAGE gel showing the purity of Avi-taggedTM CaMK1D after various purification steps. Purified CaMK1D is shown at about 40 kDa in the Ni-NTA elution, then shifted down slightly to about 37 kDa after TEV cleavage of the His6 tag. The final purified product is shown at about 37 kDa in the reverse Ni-NTA flow through.

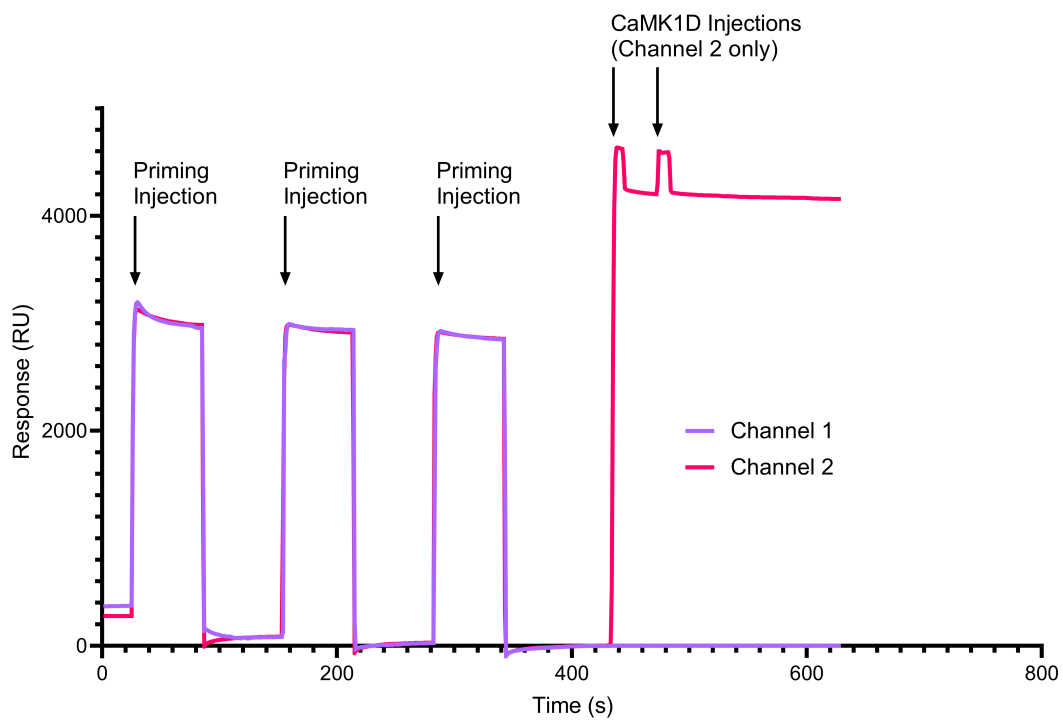


Figure 3.2: Immobilization of CaMK1D to streptavidin chip. Baseline corrected SPR response to immobilization of biotinylated AviTaggedTM CaMK1D to a streptavidin chip. CaMK1D was injected into channel 2 only, leaving channel 1 as a reference.

Table 3.1: **Summary of CaMK1D Inhibitor Binding Kinetics by SPR.**

Binding kinetic values (K_D , k_{on} and k_{off}) for inhibitor CS587, CS640 and CS861. 95% confidence intervals are provided where appropriate. N.D. = not determined.

Inhibitor	K_D (M)	k_{on} ($\text{min}^{-1}\text{M}^{-1}$)	k_{off} (min^{-1})
CS587	N.D.	N.D.	N.D.
CS640	N.D.	N.D.	N.D.
CS861	1.67×10^{-9}	$1.64 \times 10^7 \pm 1.94 \times 10^6$	$2.73 \times 10^{-2} \pm 3.40 \times 10^{-4}$

to determine kinetic constants for CS587. Using GraphPad Prism, only one response curve for 1000 nM CS587 was high enough quality to fit, and the fit produced was poor (Figure 3.3A). As this data quality is insufficient, kinetic constants were not determined. Tests with compound CS640 resulted in better curves, in which the binding stabilized at a maximum response. However, the maximum response was similar in value for concentrations from 2 to 100 nM; the maximum response should generally increase with increasing concentration (Figure 3.3B). Using the Biacore T200 analysis software, kinetic constants could not be uniquely determined, and using GraphPad Prism, only curves for 50 and 100 nM concentrations produced good curve fits. While this data quality is improved over that of CS587, it is still insufficient to reliably determine kinetic constants. For the CS861 data, the binding curves were the expected shape, reaching plateaus at both maximum binding and complete dissociation, and showed increasing maximum response with each concentration (Figure 3.3C). The BioRad T200 analysis software was able to determine kinetic constants from the aggregate data, and individual curve fitting using GraphPad Prism returned values within a similar range. Because the curve fitting was better in GraphPad Prism, the average of fits from this software are reported here. The average K_D was 1.67×10^{-9} M, or 1.67 nM. Kinetic data for CS587 and CS640 could not be determined due to poor data quality, while CS861 produced good data quality and resulted in a nanomolar level dissociation constant.

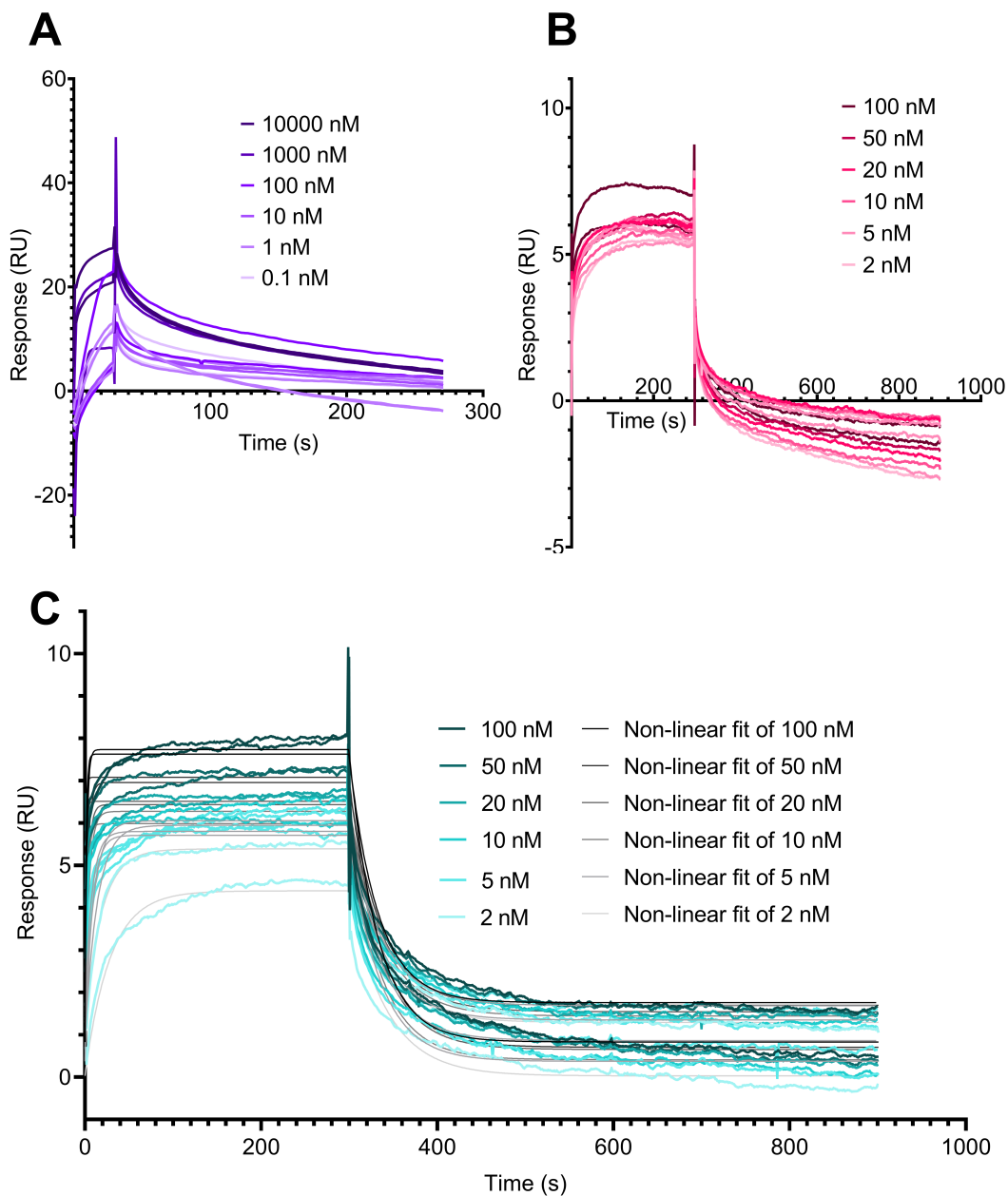


Figure 3.3: Compound binding to CaMK1D by SPR.

Reference subtracted SPR response to compounds binding to, and dissociating from, CaMK1D immobilized on a streptavidin chip. A) SPR response to 30 s binding followed by 240 s dissociation of 0.1-10 000 nM compound CS587. B) SPR response to 300 s binding followed by 600 s dissociation of 2-100 nM compound CS640. C) SPR response to 300 s binding followed by 600 s dissociation of 2-100 nM compound CS861, and curve fitting for each curve. There are two replicates for each concentration, with the exception of 1 nM compound CS587 and 5 nM compound CS640 and CS861, which each have four replicates.

3.1.3 Neurotoxicity of CaMK1D inhibitors

Neurotoxicity of CaMK1D inhibitors CS587, CS640 and CS861 was examined to determine their suitability for further studies in neurons and animals. Appropriate concentrations of inhibitor to use in these studies also needed to be chosen. These needed to be high enough to bind a significant portion of the CaMK1D population, but low enough to maintain cell viability. CaMK1D inhibitors were tested for toxicity in mouse primary neuronal cell cultures by MTT assay (Figure 3.4). In concentration ranges from 1 nM to 1 μ M in the cell culture media, no significant loss of viability was observed from any of these inhibitors (Figure 3.4 A-C). LDH assays were used as a second assay to confirm the lack of toxicity, as these indicate rupture of cell membranes rather than metabolic activity. At CS640 concentrations up to 1 μ M in the cell culture media, no significant toxicity was observed (Figure 3.4 D). However, at the concentration of 10 μ M in the cell culture media, all three inhibitors were found to be highly toxic by MTT assay. At this concentration, CS587 left less than 6 % viability, CS640 left less than 1 % viability, and CS861 left about 28 % viability (Figure 3.4 E). In one trial, CS587 seemed to increase the viability of these cells at concentrations of 1 nM and 10 nM by about 1.5 times ($p=0.0033$ and $p=0.0003$ respectively) (Figure 3.4 A, Trial 1), however this could not be repeated. From this data, it was determined that CaMK1D inhibitors could be used in media concentrations up to 1 μ M without detrimental effects on cell viability.

3.2 Neurotoxicity of A β ₁₋₄₂ oligomers

To ensure prepared A β ₁₋₄₂ oligomers were displaying similar toxicity levels as in literature[48, 96], toxicity of A β ₁₋₄₂ oligomers to primary cortical neuron cultures were tested. These experiments also helped to inform an appropriate concentration of A β ₁₋₄₂ oligomers to use for further experiments. Toxicity of A β ₁₋₄₂ oligomers at varying concentrations were tested by MTT assays (Figure 3.5). The trend of decreasing viability with increasing A β ₁₋₄₂ concentration was consistent. Variation between trials up to 30 % points was observed in the viability of cells when exposed to the same concentration of A β ₁₋₄₂ for the same time period.

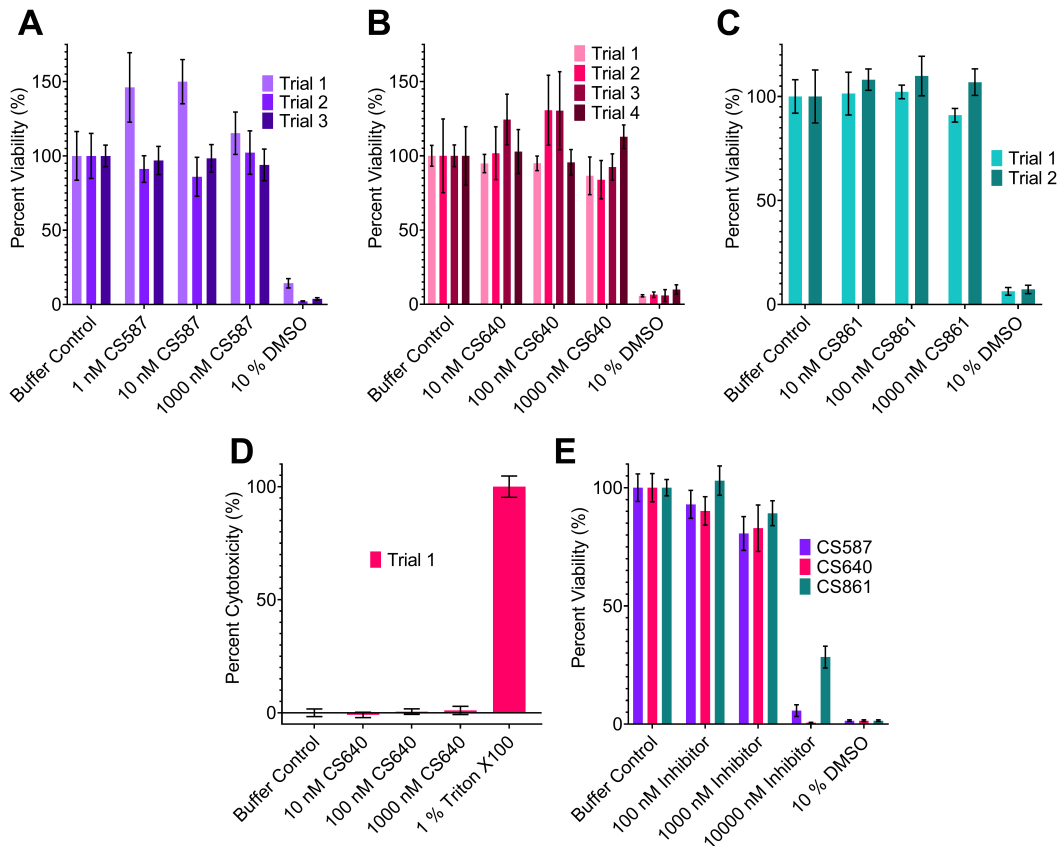


Figure 3.4: Effect of varying concentrations of CaMK1D inhibitors on primary neurons.

Viability of mouse primary cortical neurons was measured by MTT assay, and cytotoxicity was measured by LDH assay. The response from cells treated with a buffer control was normalized to 100 % viability or 0 % cytotoxicity respectively. For these assays, 10 % DMSO, or 1 % Triton X100, were used as positive controls for MTT and LDH assays respectively. A) Results of three separate MTT assay trials using CS587. B) Results of four separate MTT assay trials using CS640. C) Results of two separate MTT assay trials using CS861. D) Results of one LDH assay trial with CS640. E) Results of all three inhibitors tested at higher concentrations, up to 10 μ M, by MTT assay. Bars represent the mean of six replicates, and error bars represent standard deviation.

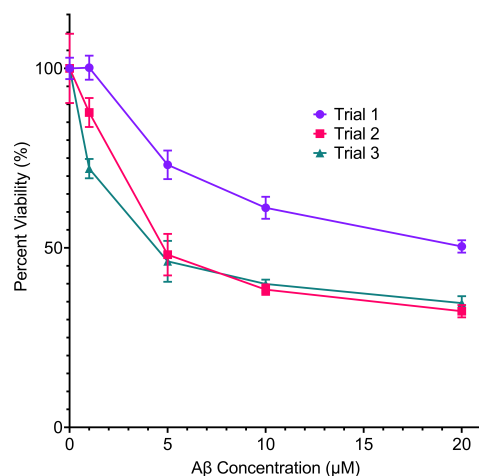


Figure 3.5: Effect of varying concentrations of Aβ₁₋₄₂ on the viability of primary neurons.

Viability of mouse primary cortical neurons was measured by MTT assay in three separate trials. Points represent the mean of six replicates, and error bars represent standard deviation.

This is expected, as variation in Aβ oligomer sizes in oligomerization experiments, and differential effects of different oligomer sizes, is well known[145], but consistency within a batch can be expected. Following a 24 h treatment, cells treated with 1 μM Aβ₁₋₄₂ retained between 66 to 100 % viability, those treated with 5 μM Aβ₁₋₄₂ retained between 42 to 76 % viability, those treated with 10 μM Aβ₁₋₄₂ retained between 35 to 64 % viability and those treated with 20 μM Aβ₁₋₄₂ retained between 30 to 53 % viability. LDH assays performed with 10 μM Aβ₁₋₄₂ resulted in 29 % cytotoxicity, consistent with the inverse of the viability range observed using MTT assays (Figure 3.10 D). Aβ₁₋₄₂ induced toxicity levels were comparable with values from literature[48, 96]. A 5-10 μM Aβ₁₋₄₂ concentration in media was chosen for use in further experiments, as these are the lowest concentrations that showed a consistent, significant reduction in viability.

3.3 Phosphorylation and cleavage of CaMK1D

3.3.1 Cleavage state of CaMK1D

Previous studies suggested that CaMK1D may be cleaved in brain samples from AD patients based on the appearance of a few 25 to 35 kDa bands and a 15 kDa band by western blot[129]. To determine whether CaMK1D is cleaved in a mouse primary neuron AD model, western blots were examined using the 350-C CaMK1D antibody. No CaMK1D fragments were observed in either control or A β ₁₋₄₂ oligomer treated mouse primary neurons; only full length CaMK1D was observed (Figure 3.6A). Since this antibody only detects amino acids from 350-C in CaMK1D, an in gel digestion and protein identification mass spectrometric analysis was performed to search for any CaMK1D fragments. Similarly, CaMK1D was detected in SDS-PAGE gel sections at the full length of CaMK1D, but not in gel sections containing smaller sized proteins (Figure 3.6B). Related CaMK proteins were also explored, resulting in the detection of γ CaMKII and β CaMKII at their expected full-length size between 50-60 kDa, and CaMK1A and CaMK1B at their expected full length size of 35-50 kDa. β CaMKII was also detected in the 20-25 kDa section. At the full length of CaMK1D, three tryptic peptides were identified, with combined 9.6 % coverage. Two of these peptides were in the conserved kinase domain region of CaMK1D, and would therefore be expected to be present in CaMK1D fragments as well, while the other overlapped the AID and CBD. While this does not guarantee that CaMK1D fragments are not present in A β ₁₋₄₂ oligomer treated mouse primary neurons, it suggests that at most there is a very low abundance of CaMK1D fragments. CaMK1D is predominantly full-length in a mouse primary neuron model of AD.

3.3.2 Phosphorylation state of CaMK1D

The phosphorylation status of kinases such as CaMK1D controls their activity, and hence is important to understanding their role in neuronal signalling and AD progression. In order to examine the potential hyperphosphorylation of CaMK1D in an AD model, mouse primary neuron cell cultures were treated with 5 μ M A β ₁₋₄₂

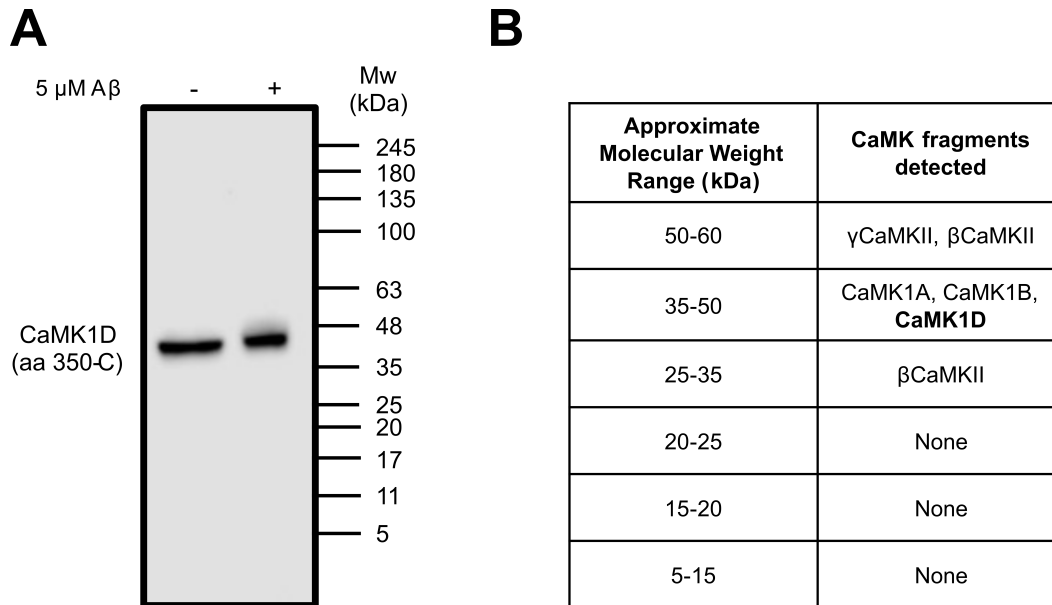


Figure 3.6: **Lack of evidence for CaMK1D fragments.**

A) A representative western blot using a CaMK1D antibody against amino acids 350-C. n = 3. B) A table showing in which molecular weight ranges CaMK fragments were detectable by in gel digestion. n = 1.

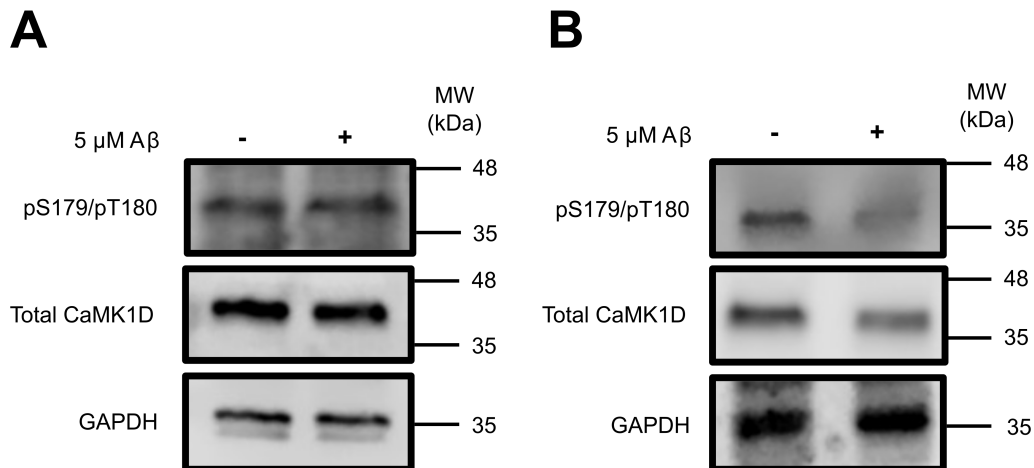


Figure 3.7: **Relative abundance of phosphorylated CaMK1D in mouse primary neuronal cell cultures.**

A) A western blot showing the relative abundance of CaMK1D phosphorylated at Ser179 and Thr180, total CaMK1D and GAPDH in the absence and presence of a 30 min 5 μ M A β_{1-42} oligomer treatment. n = 1. B) A western blot showing the relative abundance of CaMK1D phosphorylated at Ser179 and Thr180, total CaMK1D and GAPDH in the absence and presence of a 24 h 5 μ M A β_{1-42} oligomer treatment. n = 1.

oligomers, and western blots using an antibody specific for dual phosphorylation of Ser179 and Thr180 of CaMK1D as well as the 350-C CaMK1D antibody were performed on the cell lysates. When A β ₁₋₄₂ oligomer treatments lasted 30 min, these western blots revealed no clear change in CaMK1D phosphorylation levels (Figure 3.7A). When the A β ₁₋₄₂ oligomer treatments were extended to 24 h, phosphorylation levels of CaMK1D appear somewhat reduced compared to control cells (Figure 3.7B). As these experiments could only be completed once each, statistical analysis could not be completed. Thus, it is unclear how and if CaMK1D phosphorylation is altered in primary neuron cultures upon A β ₁₋₄₂ oligomer treatment. Overall, this data does not support the hyperphosphorylation of CaMK1D, but also cannot exclude the possibility of hyperphosphorylation.

3.4 Activity of CaMK1D

3.4.1 Changes to CREB phosphorylation with CaMK1D inhibitor treatment

The phosphorylation status of CREB can be indicative of the activity of CaMK1D, as it is a known CaMK1D substrate[87]. However, as CREB can be phosphorylated by other kinases as well, inhibitors for CaMK1D were used to examine CaMK1D-linked CREB phosphorylation. Western blots using a CREB antibody specific to the Ser133 phosphorylation site as well as a total CREB antibody were performed on mouse primary neurons treated with A β ₁₋₄₂ oligomers, CaMK1D inhibitor CS640, both, and neither. These revealed changes in CREB phosphorylation status (Figure 3.8). After treatment with 1 μ M CS640, CREB phosphorylation was reduced. In two out of four replicates, treatment with 5 μ M A β ₁₋₄₂ oligomers caused a substantial visual increase in CREB phosphorylation, as seen in a representative blot (Figure 3.8A). In the other two replicates, treatment with 5 μ M A β ₁₋₄₂ oligomers visibly decreased CREB phosphorylation, as seen in a representative blot (Figure 3.8B). Interestingly, when treated with both 1 μ M CS640 and 5 μ M A β ₁₋₄₂ oligomers, the level of CREB phosphorylation appears approximately equal to that of the DMSO control cells, regardless of the response to A β ₁₋₄₂ oligomer treatment alone. Be-

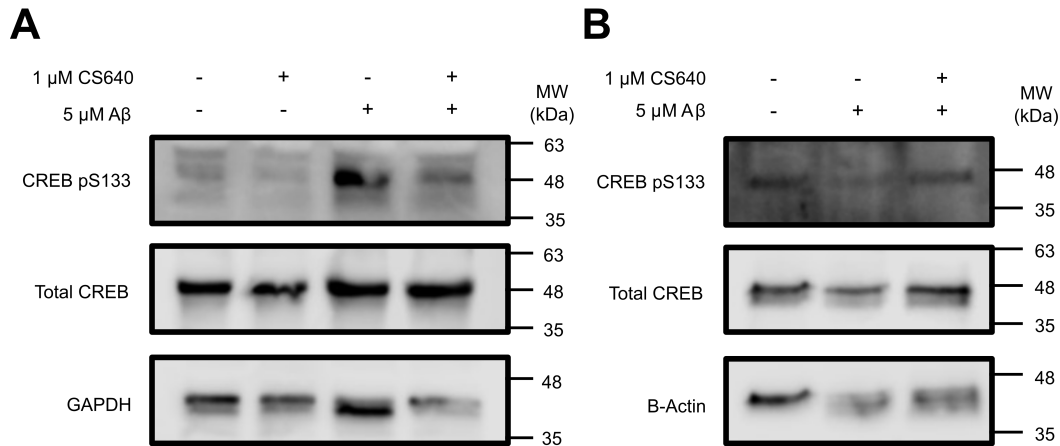


Figure 3.8: **Relative abundance of phosphorylated CREB in mouse primary neuronal cell cultures.**

A) A western blot showing the relative abundance of CREB phosphorylated at Ser133, total CREB and GAPDH in the absence and presence of 1 μM CS640 and/or 5 μM Aβ₁₋₄₂ oligomers. n = 2. B) A western blot showing the relative abundance of CREB phosphorylated at Ser133, total CREB and β-Actin in the absence and presence of 1 μM CS640 and/or 5 μM Aβ₁₋₄₂ oligomers. n = 2.

cause each of these circumstances were only observed twice, statistical analysis could not be performed, and loading controls for these blots do not appear identical. This suggests that there may be a deregulation of CaMK1D in mouse primary neurons treated with Aβ₁₋₄₂ oligomers, and that CaMK1D CS640 can neutralize this deregulation.

3.5 Effect of CaMK1D inhibitors on the progression of AD-like pathology in cell culture

3.5.1 Effect of CaMK1D inhibitors on tau phosphorylation

Hyperphosphorylation of tau is a key event in AD pathology. The effect of a CaMK1D inhibitor on tau phosphorylation was examined to investigate the involvement of CaMK1D in tau phosphorylation. Tau phosphorylation at Thr181 in mouse primary cortical neuron cultures was observed by western blotting using the AT270 antibody, and total tau was observed using the Tg5 antibody (Figure 3.9). Treatment with 1 μM CS640 for 12 h was only performed once, and is

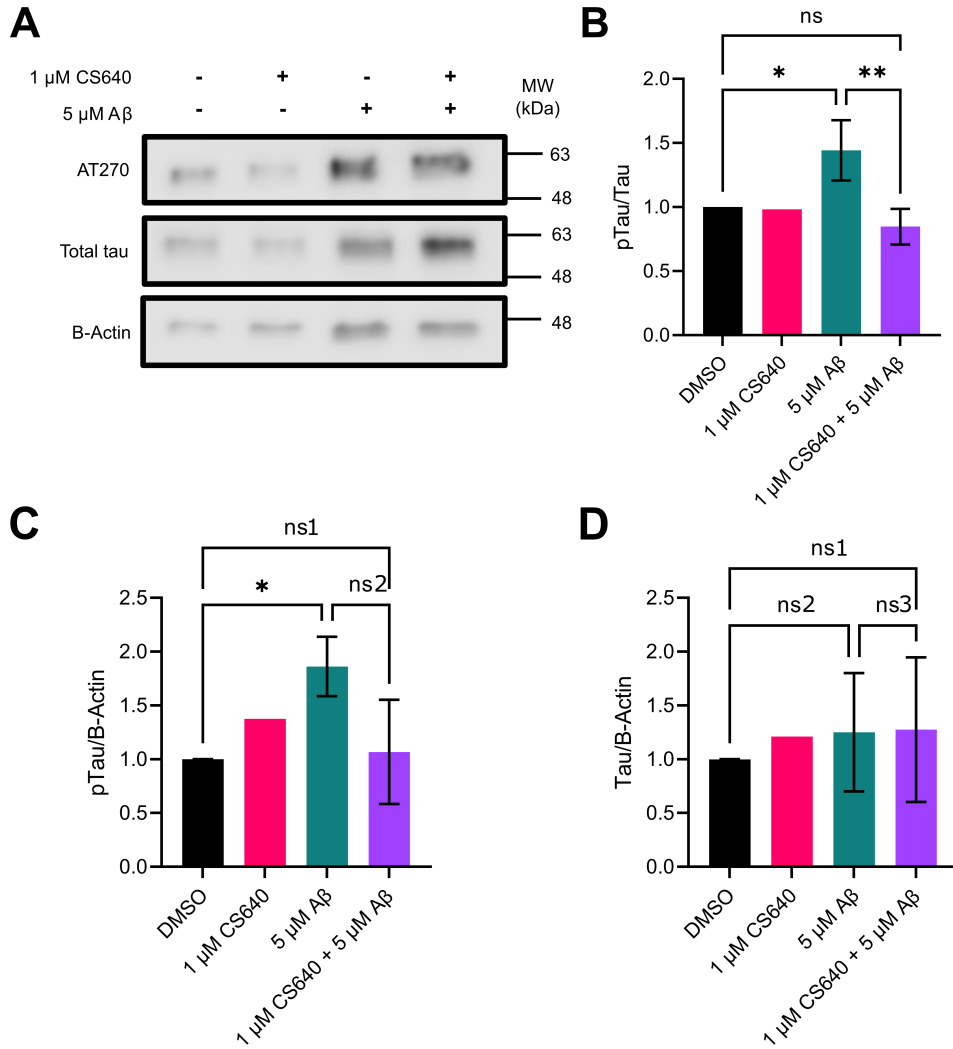


Figure 3.9: Relative abundance of phosphorylated tau in mouse primary neuronal cell cultures.

A) A representative western blot showing the relative abundance of tau phosphorylated at Thr181 (AT270), total tau and β -Actin in the absence and presence of 1 μ M CS640 and/or 5 μ M $A\beta_{1-42}$ oligomers. $n = 3$. B) Averages of the relative abundance of tau phosphorylated at Thr181 over total tau in the absence and presence of 1 μ M CS640 and/or 5 μ M $A\beta_{1-42}$ oligomers, calculated from quantifications of three replicates of western blots. $^{ns}p=0.5004$, $^*p=0.0318$, $^{**}p=0.0085$. C) Averages of the relative abundance of tau phosphorylated at Thr181 (AT270) over β -Actin with the same treatments from the same western blots. $^{ns1}p=0.9638$, $^*p=0.0387$, $^{ns2}p=0.0531$. D) Averages of the relative abundance of total tau over β -Actin with the same treatments from the same western blots. $^{ns1}p=0.7868$, $^{ns2}p=0.8192$, $^{ns3}p=0.9979$. Error bars represent standard deviation. Only one replicate of 1 μ M CS640 alone was performed, and it is thus excluded from the statistical analysis.

thus excluded from statistical analysis of these blots, though visually it did not seem to have a substantial impact on either tau phosphorylation or total tau. A 12 h treatment with 5 μM $\text{A}\beta_{1-42}$ oligomers caused an increase in the proportion of tau that is phosphorylated compared to total tau at this site of 1.45 times ($p=0.0318$) (Figure 3.9B). This increase was ablated by co-treatment over 12 h with 1 μM CS640 ($p=0.0085$). Here the proportion of tau that is phosphorylated at this site decreased to about 0.85 times the DMSO control, statistically indistinguishable from the DMSO control ($p=0.5004$). Similarly, the amount of phosphorylated tau compared to β -Actin increased by 1.86 times ($p=0.0387$) when treated with 5 μM $\text{A}\beta_{1-42}$ oligomers (Figure 3.9C), but in this case the amount of phosphorylated tau was statistically indistinguishable from the co-treatment over 12 h with 1 μM CS640 ($p=0.0531$). Here the amount of phosphorylated tau was 1.07 times the DMSO control, which is statistically indistinguishable from the DMSO control ($p=0.9638$). Though total tau levels visually appear to change with various treatments, these are indistinguishable when compared to β -Actin. This suggests that the CS640 compound was able to reduce the proportion of $\text{A}\beta_{1-42}$ oligomer induced tau phosphorylation at Thr181 compared to total tau.

3.5.2 Effect of CaMK1D inhibitors on $\text{A}\beta_{1-42}$ oligomers neurotoxicity

Neuronal death is another key event in AD, so the effect of CaMK1D inhibitors on $\text{A}\beta_{1-42}$ induced toxicity in primary neurons was examined. MTT and LDH assays were performed on mouse primary neurons treated with $\text{A}\beta_{1-42}$ oligomers in the presence of varying concentrations of CaMK1D inhibitors CS587, CS640 and CS861 (Figure 3.10).

The CS587 compound was tested for effect on cell viability in the presence of 10 μM $\text{A}\beta_{1-42}$ oligomers. In one trial, the viability of cells treated with both 10 nM CS587 and 10 μM $\text{A}\beta_{1-42}$ oligomers was higher than cells treated with 10 μM $\text{A}\beta_{1-42}$ oligomers alone by about 1.24 times ($p=0.0064$)(Figure 3.10 A(1)). In all other trials, and at all other concentrations (1 nM to 1 μM), CS587 did not have a significant effect on cells viability in the presence of 10 μM $\text{A}\beta_{1-42}$ oligomers, so

it is likely that the first trial was a statistical anomaly (Figure 3.10 A).

The CS640 compound was tested for effect on cell viability in the presence of both 10 and 5 μM $\text{A}\beta_{1-42}$ oligomers. In one trial, the viability of cells treated with both 1 μM CS640 and 10 μM $\text{A}\beta_{1-42}$ oligomers was higher than cells treated with 10 μM $\text{A}\beta_{1-42}$ oligomers alone by about 1.4 times ($p=0.0009$)(Figure 3.10 B 10 μM $\text{A}\beta_{1-42}$), but this could not be repeated in further trials. In all other trials, and at all other concentrations (10 nM to 1 μM), CS640 did not have a significant effect on cell viability in the presence of either 10 μM $\text{A}\beta_{1-42}$ oligomers or 5 μM $\text{A}\beta_{1-42}$ oligomers, so it is likely that the first trial was a statistical anomaly (Figure 3.10 B). Similarly, when tested with LDH assays, cytotoxicity of cells treated with 10 μM $\text{A}\beta_{1-42}$ oligomers did not significantly differ from those treated with both 10 μM $\text{A}\beta_{1-42}$ oligomers and varying concentrations (10 nM to 1 μM) of CS640 (Figure 3.10 D).

The CS861 compound was also tested for effect on cell viability in the presence of both 10 and 5 μM $\text{A}\beta_{1-42}$ oligomers. In all trials, and at all concentrations of both $\text{A}\beta_{1-42}$ oligomers and CS861 (10 nM to 1 μM), there was no significant difference in viability between $\text{A}\beta_{1-42}$ oligomers alone and $\text{A}\beta_{1-42}$ oligomers and CS861 together (Figure 3.10 C).

Overall, this data suggests that CaMK1D inhibitors are not able to consistently protect mouse primary neurons from $\text{A}\beta_{1-42}$ induced toxicity.

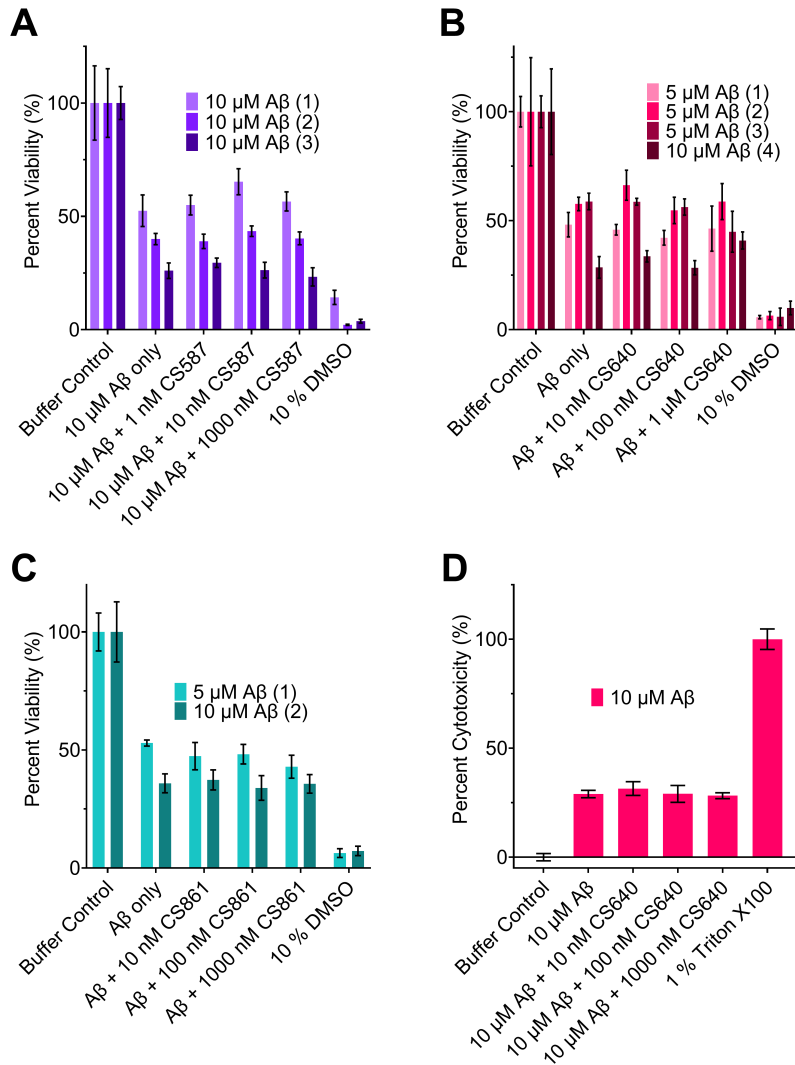


Figure 3.10: Effect of varying concentrations of CaMK1D inhibitors on the viability of primary neurons treated with Aβ₁₋₄₂ oligomers.

Viability of mouse primary cortical neurons was measured by MTT assay, and cytotoxicity was measured by LDH assay. The response from cells treated with a buffer control was normalized to 100 % viability or 0 % cytotoxicity respectively. For these assays, 10 % DMSO, or 1 % Triton X100, were used as positive controls for MTT and LDH assays respectively. Trial numbers are indicated in parentheses. A) Results of three separate MTT assay trials using CS587 and 10 μM Aβ. B) Results of three separate MTT assay trials using CS640 and 5 μM Aβ, as well as one trial using 10 μM Aβ₁₋₄₂. C) Results of two separate MTT assay trials using CS861, one with 5 μM Aβ₁₋₄₂ and the other with 10 μM Aβ₁₋₄₂. D) Results of one LDH assay trial with CS640 and 10 μM Aβ₁₋₄₂. Bars represent the mean of six replicates, and error bars represent standard deviation.

Chapter 4

Discussion

4.1 Properties of CaMK1D inhibitors

4.1.1 CaMK1D inhibitors have nanomolar level K_D values

The AviTaggedTM CaMK1D protein was successfully purified to >80 % purity. Since the biotinylation of an AviTagTM by the BirA enzyme is a highly specific reaction, and the biotin-streptavidin interaction is also highly specific[146], this purity was sufficient to ensure negligible binding of contaminant proteins to the SPR chip.

The K_D value for CaMK1D inhibitor CS587 could not be determined by SPR (Table 4.1). Binding and dissociation times used were insufficient to reach a plateau for maximum binding or for complete dissociation respectively. Unfortunately, practical considerations prevented the repetition of these experiments. Published IC_{50} values for CS587 are 31 nM and 8 nM for enzymatic and cellular assays, respectively[137] (Table 4.1). While the K_D could not be reported, the IC_{50} values indicate that only nanomolar levels of CS587 are required to impact the activity of the protein.

Similarly, the K_D value for CS640 could not be determined due to poor data quality, though for a different reason. In these experiments, enough time was provided for maximum binding and complete dissociation plateaus to be reached. However, for this data, increasing inhibitor concentrations did not lead to increasing maximum response as expected. This may be due to the compound aggregating in solution. This aggregation would likely be more pronounced in the

higher concentrations of CS640, reducing the amount of compound available to bind CaMK1D, and causing the higher concentrations to behave similarly to the lower concentrations. Published enzymatic and cellular IC_{50} values were 8 nM and 11 nM, respectively[137] (Table 4.1). Again, while the K_D could not be reported, the IC_{50} values indicate that only nanomolar levels of CS640 are required to impact the activity of the protein.

For CS861, the K_D value was 1.67 nM (Table 4.1). This data plateaued at maximum responses and complete dissociations, and showed increasing maximum response over increasing inhibitor concentrations. No IC_{50} values have yet been published for this compound. However, structurally, the portion of CS861 which binds to the ATP binding pocket of CaMK1D is identical to CS640 (Figure 4.1). Cellular IC_{50} values from CS640 are not useful in this case, because CS861 also functions to bring about the degradation of CaMK1D by the proteasome, and is therefore not exclusively a competitive inhibitor. However, the enzymatic, *in vitro*, IC_{50} values can be expected to be similar between these two compounds based on their structural similarity. The enzymatic IC_{50} for CS640 is 8 nM[137]. In this case, the estimated IC_{50} value is greater than the K_D , satisfying the Cheng-Prusoff equation[147]. This equation states that for a competitive inhibitor, the IC_{50} should always be greater than the K_D value of the inhibitor, which is the case here, assuming the enzymatic IC_{50} values are similar between CS640 and CS861. This provides further confidence in the accuracy of the determined K_D value.

4.1.2 CaMK1D inhibitors are non-neurotoxic up to 1 μ M concentrations

Originally, there were concerns that these particular kinase inhibitors could potentially exhibit toxicity toward neuronal cells, even at low concentrations. CaMK1D is expressed most highly in the brain during early development and is important for basal dendritic growth[123], these inhibitors have nanomolar level IC_{50} and K_D values for CaMK1D, and the inhibitors can affect other members of the CaMKI family[137]. Thus, it was reasonable to expect that they may be toxic to neuronal cells, particularly on the primary neurons used here, as they are derived from de-

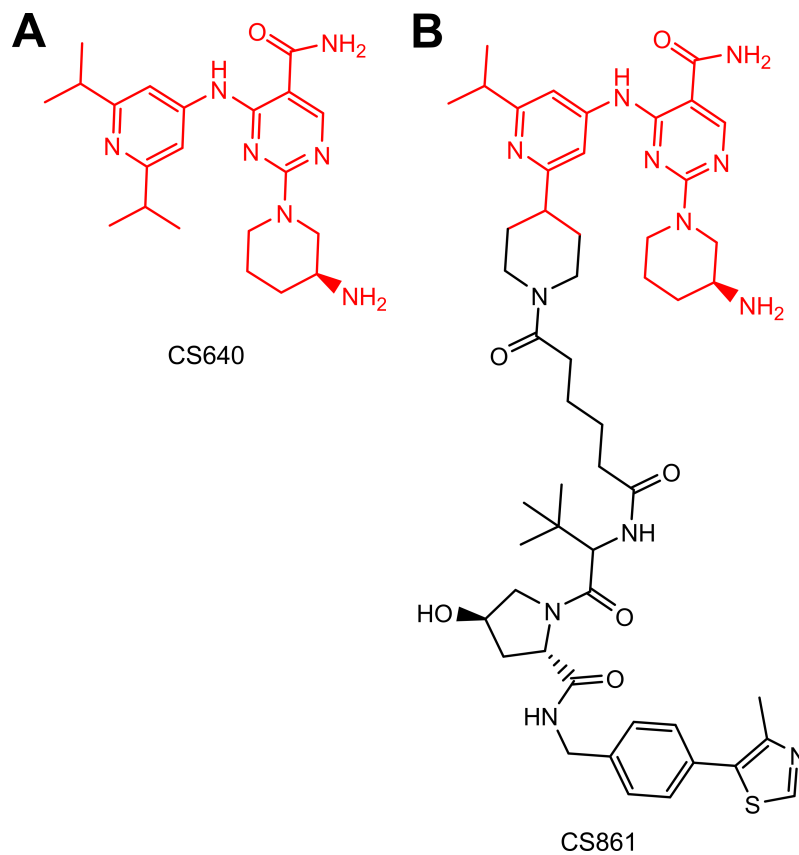


Figure 4.1: **Comparison of the structures of CS640 and CS861.**

A) The structure of CS640. B) The structure of CS861. The identical portion of the two compounds is highlighted in red.

Table 4.1: **Summary of CaMK1D Inhibitor Properties.**

Dissociation constants (K_D), IC_{50} values, and maximum recommended concentrations in cell culture for inhibitor CS587, CS640 and CS861.

N.D. = not determined. IC_{50} values are from Fromont et al. 2020[137].

Inhibitor	K_D (nM)	IC_{50} - enzymatic (nM)	IC_{50} - cellular (nM)	Maximum recommended concentration (nM)
CS587	N.D.	31	8	1000
CS640	N.D.	8	11	1000
CS861	1.67	Unknown	Unknown	1000

veloping brains. However, this was not the case. At levels in media up to $1\ \mu\text{M}$, none of the inhibitors showed any significant neurotoxicity. However, virtually all neurons were killed by $10\ \mu\text{M}$ CS587 and CS640, and the majority were killed by $10\ \mu\text{M}$ CS861 (Figure 3.4). Given that the IC_{50} and K_D values for all three inhibitors were in the nanomolar range, concentrations up to $1\ \mu\text{M}$ should be more than enough to be effective for use in cell culture experiments. These results can be used to inform dosage in future animal studies; dosages used previously remained below $10\ \mu\text{M}$ *in vivo*, with the maximum concentration reaching $3\ \mu\text{M}$ *in vivo*[137]. Naturally, a lack of neurotoxicity is an important attribute in a compound being used for research on a neurodegenerative disease such as AD. These inhibitors can be confidently used in further cell-based AD models, at concentrations of $1\ \mu\text{M}$ and lower (Table 4.1). Researchers can proceed with more confidence in animal studies, whether focusing on breast cancer, diabetes, or AD, as neurotoxicity concerns have been addressed.

4.2 CaMK1D is neither hyperphosphorylated nor cleaved in $A\beta_{1-42}$ -treated mouse primary neurons

Based on data from Riascos et al. 2014, CaMK1D was expected to be cleaved and therefore hyperphosphorylated in AD (Figure 1.6)[129]. Removal of the AID from

the kinase domain could result in CaMKs, which activate CaMK1D by phosphorylating Thr180, having constant access to the activation loop[121]. In mouse primary neurons, neither cleavage of CaMK1D (Figure 3.6), nor a significant increase in phosphorylation level of Ser179 and Thr180 was seen when treated with A β ₁₋₄₂ oligomers (Figure 3.7).

Only full length CaMK1D was detected by western blot, giving the first evidence that CaMK1D may not be cleaved in these cells. The antibody used here, specific to amino acids 350 to the C terminus, only detects the widely expressed CaMK1D splice variant, and thus avoids confusing splice variants with cleavage products. However, this antibody detects the section of CaMK1D that was expected to be cleaved off of the protein, and a small protein fragment such as this is likely to be quickly degraded in a cell. If this was the case, fragments would not be detectable by western blot with this antibody under these conditions, though a proteasome inhibitor treatment may help to prevent this degradation. Mass spectrometry was thus used to search for fragments more generally, but no fragments were detected by this method either. Based on this data, there is no evidence that CaMK1D is cleaved in mouse primary neurons. If fragments exist, they are in quantities that are too small to detect. While this seems to contradict Riascos et al. 2014[129], upon further inspection, there is another explanation for the smaller, unidentified bands shown in the published western blot. The antibody used in the published experiment is specific to a sequence around amino acid 150 in CaMK1D, but the exact sequence is proprietary. Amino acid 150 is within the conserved kinase domain of CaMK1D, and the sequence around it is highly conserved between the CaMKI family, and is somewhat conserved between other CaMK proteins as well. Thus, it is possible that the extra bands seen are splice variants and/or cleavage products of other CaMK proteins. Taking a closer look at the mass spectrometry data, β CaMKII was identified in the approximately 25-35 kDa size range. Three tryptic peptides were identified, with one of these covering the conserved region corresponding to CaMK1D amino acid 150. Depending on the length and exact location of the antibody's epitope, conservation in this region is up to 100 % for a span of ten amino acids. This could align with the larger size "fragments" seen

in the published blot. However, this still does not explain the 15 kDa band. No CaMK proteins were identified in any smaller mass spectrometry sections. If this is a cleavage product, either of CaMK1D or other CaMKI proteins, it would not likely be an active protein. The conserved kinase domain itself is 29 kDa in size, so only half of it could be retained in a 15 kDa protein. This would probably not be sufficient to be active. The data presented here does not support the cleavage of CaMK1D in mouse primary neurons.

The amount of dually phosphorylated CaMK1D did not change substantially in A β ₁₋₄₂ treated mouse primary neurons, indicating that CaMK1D is not dually phosphorylated in the activation loop in this AD model. However, this only represents the dually phosphorylated species of CaMK1D, as the antibody used in these experiments is specific for the dually phosphorylated state of the protein. It can be reasonably expected that changes in the phosphorylation level of the dually phosphorylated species would be related to the phosphorylation levels of singly phosphorylated species, as the latter is likely necessary to create the former. However, while a lack of amplification of the dually phosphorylated species suggests that the singly phosphorylated species are also not amplified, it does not prove this. It is possible that species of CaMK1D either phosphorylated at Ser179 or Thr180 alone are amplified. Unfortunately, antibodies specific to the individual phosphorylation sites are not currently widely available or effective, so visualizing these species is difficult. As the activity levels of various phosphorylated CaMK1D species have not been reported in literature, it is currently unclear whether the dually phosphorylated species, or a singly phosphorylated species, demonstrates the highest activity. Thus it is still possible that there is a hyperphosphorylated, hyperactive species of CaMK1D that cannot be seen in these results, though this is speculative and unlikely. These results overall do not support the hyperphosphorylation of CaMK1D in an A β ₁₋₄₂ treated mouse primary neuron system, but also do not eliminate the possibility.

While this data suggests no changes to cleavage of CaMK1D or the quantity of CaMK1D that is dually phosphorylated in the activation loop, it should be noted that CaMK1D has various other potential heterogeneities that have not been

explored here. These heterogeneities include phosphorylation at various other sites[148], which may have regulatory roles in the conformation of the protein, its ability to bind CaM, its ability to bind substrates, etc. CaMK1D can also be acetylated at Lys146 and Lys174[148], with Lys174 being close to the activation loop phosphorylation sites. These also have the potential to regulate the activity of the protein. The localization of the protein could also influence its role; CaMK1D has been shown to localize to the nucleus[87], cytoplasm[87], and membranes[149]. While most research, including this work, have focused on activation loop phosphorylation and CaM binding to regulate CaMK1D, there are other potential factors that could influence the activities of CaMK1D in normal and diseased tissues.

4.3 Inhibitors for CaMK1D ablate $A\beta_{1-42}$ -induced changes to CREB phosphorylation

CREB phosphorylation status can be indicative of CaMK1D activity, as CREB is a known CaMK1D substrate[87]. The majority of data examining CREB phosphorylation at Ser133 in various AD models has shown a reduction in CREB phosphorylation [86, 90–92], however, some studies have shown an increase in CREB phosphorylation[93]. Interestingly, here each were observed in half of the replicates. The degree of change in CREB phosphorylation seen in each case was consistent with the respective previous studies[90, 93]. It is possible that these polarized results are due to inconsistencies in the $A\beta_{1-42}$ oligomer composition, as variable oligomer lengths can produce different results in AD models[145]. This may also be due to inconsistencies in primary cultures, due to variations in confluency, glial contamination, etc. or in the mice themselves, due to variations in stress, precise age of the pups, etc. Perhaps even more interestingly, CaMK1D inhibitor CS640 was able to ablate $A\beta_{1-42}$ -induced changes in CREB phosphorylation regardless of whether CREB phosphorylation was increased or decreased. In the case that $A\beta_{1-42}$ causes an increase in CREB phosphorylation, this is an expected result. If the increased CREB phosphorylation is due to aberrant activity of CaMK1D, intuitively, adding CaMK1D inhibitors should reduce CREB phosphorylation. This

is what is seen in the case of $A\beta_{1-42}$ -induced increased CREB phosphorylation. In the case of $A\beta_{1-42}$ -induced decreased CREB phosphorylation, it could be expected that CaMK1D inhibitors may reduce the phosphorylation of CREB even further. However, this was not the case experimentally. CaMK1D inhibitor CS640 actually caused an increase in CREB phosphorylation back to control levels. This may be due to so far unknown activity of CaMK1D or other CaMKI family members. CaMK1D is not a particularly well studied enzyme, and may have unknown substrates, while CREB is phosphorylated at Ser133 by numerous kinases. There may be a pathway in which CaMK1D activity indirectly leads to reduced activity of another CREB kinase, or inversely, leads to increased activity of a CREB phosphatase. It is also possible that this is the case for another CaMKI family member, as these inhibitors would reduce their activity as well. CaMK1 α activity can also lead to the phosphorylation of CREB through the MEK/ERK pathway[150], but there are no known pathways involving the CaMKI family where inhibiting that pathway would increase CREB activation. Regardless of how CREB phosphorylation changes with $A\beta_{1-42}$ treatment, CaMK1D inhibitor CS640 is able to ablate those changes.

4.4 CaMK1D inhibitors reduce tau phosphorylation, but not neuron death, in $A\beta_{1-42}$ treated cell cultures

Increased tau phosphorylation is a well studied AD indicator, and it is temporally correlated with brain structure changes by MRI in AD patients[50]. Here, CS640 was able to ablate the proportion of $A\beta_{1-42}$ -induced tau phosphorylation at Thr181 compared to total tau in mouse primary neurons. The total amount of $A\beta_{1-42}$ -induced tau phosphorylation at Thr181 however, could not be ablated. Nonetheless, it should be noted that the p-value observed comparing $A\beta_{1-42}$ oligomer treated, and $A\beta_{1-42}$ and CS640 treated primary neurons was 0.0531, which is very near the $p < 0.05$ cut off used here to indicate statistical significance. If for example, a 90 % confidence interval was used instead of a 95 % confidence interval, these re-

sults could have been categorized as statistically significant. This suggests that if more replicates were completed, this data could also show a significant difference at the confidence interval used here.

The phosphorylation site examined here, Thr181, is an early marker of AD which has been suggested as a cerebrospinal fluid diagnostic marker of AD[151], and has been previously shown to have increased phosphorylation induced by A β ₁₋₄₂ oligomer treatment. The increase in tau phosphorylation observed here is consistent with previous results[48, 96]. Prevention of an increased proportion of tau phosphorylation in these cultures indicates that this compound can, to some extent, attenuate the development of AD pathology in cell culture. This suggests that CaMK1D is involved in a pathway that leads to phosphorylation of tau at Thr181, an AD marker, and that attenuation of CaMK1D activity can prevent this.

Unfortunately, while reduced tau phosphorylation is promising, it was not paired with improved cell viability. In AD, and in cell culture, A β ₁₋₄₂ oligomers are neurotoxic, and A β ₁₋₄₂-induced toxicity observed here was consistent with previous results (Figure 3.5)[41–43, 48, 96]. Although inhibition of CaMK1D clearly has an impact on tau phosphorylation at Thr181, alone this was not sufficient to protect the cells from A β ₁₋₄₂-induced toxicity. This is not surprising, given that tau contains about 80 potential phosphorylation sites, many of which are AD-linked, and is phosphorylated by many established kinases. Reduction in phosphorylation of tau at one site does not necessarily predict the overall hyperphosphorylation level. Additionally, other downstream effects of A β ₁₋₄₂ treatment could cause cell death. Together, these results suggest that while inhibition of CaMK1D is not sufficient alone to combat AD related neuron death, it does effectively lower tau phosphorylation at Thr181.

A simplified model of how CaMK1D fits into an AD pathway is provided in Figure 4.2.

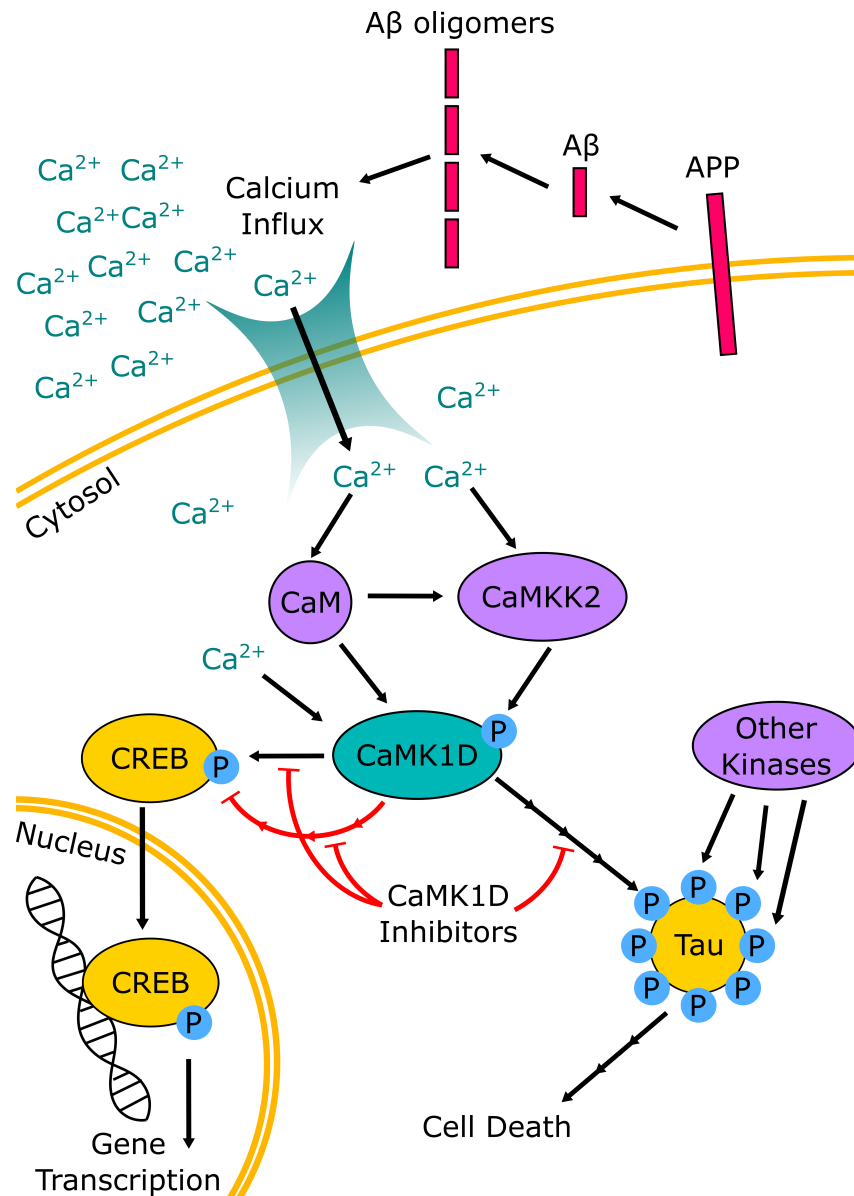


Figure 4.2: **Model of CaMK1D's involvement in AD.**

APP processing produces A β , which oligomerizes and causes an influx of Ca²⁺ into the cell. The Ca²⁺ activates CaM and CaMKK2, which activate CaMK1D. CaMK1D phosphorylates CREB at Ser133. Through an unknown pathway, CaMK1D also prevents CREB phosphorylation. CaMK1D also lead to tau phosphorylation at Thr181 through an unknown pathway. CaMK1D inhibitors interfere with CREB phosphorylation, the prevention of CREB phosphorylation, and also tau phosphorylation. However, these inhibitors do not prevent cell death, potentially due to the contributions of other tau kinases. Note that this does not depict a comprehensive AD pathway. Adapted from Marambaud et al. 2009[152].

Chapter 5

Conclusions and Future Directions

5.1 Conclusions

The work in this thesis explores the role of CaMK1D in AD, and the properties and effects of CaMK1D inhibitors. While much remains to be discovered, the three main hypotheses have been addressed, to some extent.

The first hypothesis, that inhibitors for CaMK1D can be used in cell culture experiments at effective concentrations with limited toxicity, was true for mouse primary neuron cell cultures. The IC_{50} and K_D values for CaMK1D inhibitors are all in the nanomolar range, while up to 1 μM of each inhibitor can be used with no observed toxicity. At this concentration, CS640 has an impact on both CREB and tau phosphorylation, indicating that the concentration is sufficient to observe an effect.

Contrary to the second hypothesis, CaMK1D does not appear to be cleaved or hyperphosphorylated in a mouse primary neuron culture model of AD, though there is room for further exploration in this area. Neither western blot, nor mass spectrometry of cell extracts showed any CaMK1D cleavage. Phosphorylation of CaMK1D at Ser179/Thr180 did not change significantly with $A\beta$ treatment. There is no evidence in this thesis to support the cleavage or hyperphosphorylation of CaMK1D, but there is also insufficient evidence to reject this hypothesis.

Finally, inhibitors for CaMK1D can alter the progression of AD-like pathology

in A β treated mouse primary neurons. These inhibitors ablate A β induced changes in both CREB phosphorylation at Ser133 and tau phosphorylation at Thr181. However, they did not prevent A β induced toxicity to the cells. These inhibitors are able to prevent aspects of AD in primary cell culture, but ultimately do not prevent neuron death.

5.2 Future Directions

Future studies on the role of CaMK1D in AD will aim to expand knowledge of the pathways involved in AD, eventually leading to improved treatments that slow, halt, or reverse the progression of the disease. There is much left to be explored in this space. Our collaborators have been continuously working on improving and refining the CaMK1D inhibitors, with the goal of generating more specific and effective compounds. These would be ideal for further studies, to eliminate cross-reactivity with other CaMKI family members. Further efforts in inhibitor development should also include optimization of blood brain barrier permeability of these compounds, as the current compounds were designed for TNBC and diabetes studies[137], and thus were not intended to cross the blood brain barrier. These compounds could also be evaluated for membrane permeability, and for CS861 in particular, ubiquitination of CaMK1D could be examined as a marker of membrane permeability. Ideally, these compounds would be characterized kinetically by more than one technique; isothermal titration calorimetry experiments are currently underway for the compounds used here.

Further studies of CaMK1D itself would help in the exploration of its role in AD. Much remains unknown regarding CaMK1D and its roles and regulation in both healthy and diseased states. Preliminary data from western blots and size exclusion chromatography performed without reducing agents have suggested that a portion of endogenous CaMK1D may exist as a disulphide-linked dimer, and our collaborators are exploring this in depth. Additionally, while the activation loop phosphorylation sites Ser179 and Thr180 are both known to be phosphorylated[113, 153], the individual and combined roles of the two sites is yet to be fully

explored. In order to explore this more thoroughly, antibodies specific for the individual phosphorylation sites should be developed; collaborators are currently working on this as well. Preliminary bioinformatics studies have also identified potential membrane binding sites on CaMK1D, which are now being explored experimentally.

There is much left to be discovered regarding CaMK1D and its role in AD, and questions were raised by the work completed in this thesis. Regarding the phosphorylation and cleavage state of CaMK1D, it would be beneficial to examine CaMK1D in human cells rather than mouse, and, ideally, brain samples from control and AD patients. Inhibitor based experiments would benefit from comparison to siRNA specific for CaMK1D over other CaMKI family members. Further AD-like indicators could also be explored in cell culture, such as other tau phosphorylation sites, tau aggregation and localization, and specifically apoptotic cell death. It would also be beneficial to repeat western blotting experiments shown in this thesis using ELISA, for more robust quantification. Localization of CaMK1D in AD could also be examined, to explore potential parallels with CaMKII regulation in AD.

References

1. World Health Organization. *Towards a dementia plan: a WHO guide* technical report (2018).
2. McKhann, G. M. *et al.* The diagnosis of dementia due to Alzheimer's disease: Recommendations from the National Institute on Aging-Alzheimer's Association workgroups on diagnostic guidelines for Alzheimer's disease. English. *Alzheimer's & dementia : the Journal of the Alzheimer's Association* **7**, 263–269 (May 2011).
3. Jack Jr, C. R. *et al.* NIA-AA research framework: toward a biological definition of Alzheimer's disease. *Alzheimer's & Dementia: The Journal of the Alzheimer's Association* **14**, 535–562 (2018).
4. Chávez-Gutiérrez, L. & Szaruga, M. Mechanisms of neurodegeneration - Insights from familial Alzheimer's disease. *Seminars in Cell & Developmental Biology* **105**, 75–85 (2020).
5. Maurer, K., Volk, S. & Gerbaldo, H. Auguste D and Alzheimer's disease. *The Lancet*, 1546–1549 (1997).
6. Maurer, K. in *Alzheimer: 100 Years and Beyond* 13–34 (Springer, 2006).
7. Gauthier, S. *et al.* Recommendations of the 4th Canadian Consensus Conference on the Diagnosis and Treatment of Dementia (CCCDTD4). *Canadian geriatrics journal : CGJ* **15**, 120–126 (Dec. 2012).
8. Custodio, N. *et al.* Mixed dementia: A review of the evidence. *Dementia & neuropsychologia* **11**, 364–370 (2017).
9. James, B. D. *et al.* TDP-43 stage, mixed pathologies, and clinical Alzheimer's-type dementia. *Brain* **139**, 2983–2993 (2016).
10. Hyman, B. T. & Trojanowski, J. Q. Editorial on Consensus Recommendations for the Postmortem Diagnosis of Alzheimer Disease from the National Institute on Aging and the Reagan Institute Working Group on Diagnostic Criteria for the Neuropathological Assessment of Alzheimer Disease. *Journal of Neuropathology & Experimental Neurology* **56**, 1095–1097 (1997).
11. Mirra, S. S. *et al.* The Consortium to Establish a Registry for Alzheimer's Disease (CERAD). *Neurology* **41**, 479–479 (1991).
12. Braak, H. & Braak, E. Staging of alzheimer's disease-related neurofibrillary changes. *Neurobiology of Aging* **16**, 271–278 (1995).

13. Hardy, J. A. & Higgins, G. A. Alzheimer's Disease: The Amyloid Cascade Hypothesis. *Science* **256**, 184–185 (1992).
14. Selkoe, D. J. & Hardy, J. The amyloid hypothesis of Alzheimer's disease at 25 years. *EMBO molecular medicine* **8**, 595–608 (2016).
15. Maccioni, R. B., Fariás, G., Morales, I. & Navarrete, L. The Revitalized Tau Hypothesis on Alzheimer's Disease. *Archives of Medical Research* **41**, 226–231 (2010).
16. Khachaturian, Z. S. Calcium Hypothesis of Alzheimer's Disease and Brain Aging. *Annals of the New York Academy of Sciences* **747**, 1–11 (1994).
17. Berridge, M. J. Calcium hypothesis of Alzheimer's disease. *Pflügers Archiv-European Journal of Physiology* **459**, 441–449 (2010).
18. Cameron, B. & Landreth, G. E. Inflammation, microglia, and Alzheimer's disease. *Neurobiology of disease* **37**, 503–509 (2010).
19. Coppede, F. & Migliore, L. DNA damage and repair in Alzheimer's disease. *Current Alzheimer Research* **6**, 36–47 (2009).
20. Nixon, R. A. & Yang, D.-S. Autophagy failure in Alzheimer's disease-locating the primary defect. *Neurobiology of disease* **43**, 38–45 (2011).
21. Nixon, R. A. & Cataldo, A. M. Lysosomal system pathways: genes to neurodegeneration in Alzheimer's disease. *Journal of Alzheimer's Disease* **9**, 277–289 (2006).
22. Yang, Y., Mufson, E. J. & Herrup, K. Neuronal cell death is preceded by cell cycle events at all stages of Alzheimer's disease. *Journal of Neuroscience* **23**, 2557–2563 (2003).
23. Zhu, X. *et al.* Mitochondrial abnormalities and oxidative imbalance in Alzheimer disease. *Journal of Alzheimer's Disease* **9**, 147–153 (2006).
24. Ferreira, S. T., Clarke, J. R., Bomfim, T. R. & De Felice, F. G. Inflammation, defective insulin signaling, and neuronal dysfunction in Alzheimer's disease. *Alzheimer's & Dementia: The Journal of the Alzheimer's Association* **10**, S76–S83 (2014).
25. Swerdlow, R. H. & Khan, S. M. A "mitochondrial cascade hypothesis" for sporadic Alzheimer's disease. *Medical hypotheses* **63**, 8–20 (2004).
26. Jorm, A. F. & Jolley, D. The incidence of dementia: a meta-analysis. *Neurology* **51**, 728–733 (1998).
27. Corrada, M. M., Brookmeyer, R., Paganini-Hill, A., Berlau, D. & Kawas, C. H. Dementia incidence continues to increase with age in the oldest old: the 90+ study. *Annals of neurology* **67**, 114–121 (2010).
28. Corder, E. H. *et al.* Gene Dose of Apolipoprotein E Type 4 Allele and the Risk of Alzheimer's Disease in Late Onset Families. *Science* **261**, 921–923 (Aug. 1993).

29. Corder, E. H. *et al.* Protective effect of apolipoprotein E type 2 allele for late onset Alzheimer disease. *Nature Genetics* **7**, 180–184 (1994).
30. Norton, S., Matthews, F. E., Barnes, D. E., Yaff, K. & Brayne, C. Potential for primary prevention of Alzheimer’s disease: an analysis of population-based data. *The Lancet Neurology* **13**, 788–794 (2014).
31. Selkoe, D. J. The Molecular Pathology of Alzheimer’s Disease. *Neuron* **6**, 487–498 (1991).
32. Hardy, J. & Allsop, D. Amyloid deposition as the central event in the aetiology of Alzheimer’s disease. *Trends in Pharmacological Sciences* **12**, 383–388 (1992).
33. Beyreuther, K. & Masters, C. L. Amyloid Precursor Protein (APP) and β A4 Amyloid in the Etiology of Alzheimer’s Disease: Precursor- Product Relationships in the Derangement of Neuronal Function. *Brain Pathology* **1**, 241–251 (1991).
34. Asai, M. *et al.* Putative function of ADAM9, ADAM10, and ADAM17 as APP α -secretase. *Biochemical and biophysical research communications* **301**, 231–235 (2003).
35. Zhang, Y., Thompson, R., Zhang, H. & Xu, H. APP processing in Alzheimer’s disease. *Molecular brain* **4**, 1–13 (2011).
36. O’Brien, R. J. & Wong, P. C. Amyloid precursor protein processing and Alzheimer’s disease. *Annual review of neuroscience* **34**, 185–204 (2011).
37. Hussain, I. *et al.* Identification of a novel aspartic protease (Asp 2) as β -secretase. *Molecular and Cellular Neuroscience* **14**, 419–427 (1999).
38. Kakuda, N. *et al.* Equimolar production of amyloid β -protein and amyloid precursor protein intracellular domain from β -carboxyl-terminal fragment by γ -secretase. *Journal of Biological Chemistry* **281**, 14776–14786 (2006).
39. Takami, M. *et al.* γ -Secretase: successive tripeptide and tetrapeptide release from the transmembrane domain of β -carboxyl terminal fragment. *Journal of Neuroscience* **29**, 13042–13052 (2009).
40. Meisl, G. *et al.* Differences in nucleation behavior underlie the contrasting aggregation kinetics of the A β 40 and A β 42 peptides. *Proceedings of the National Academy of Sciences* **111**, 9384–9389 (2014).
41. Kirkitadze, M. D., Bitan, G. & Teplow, D. B. Paradigm shifts in Alzheimer’s disease and other neurodegenerative disorders: the emerging role of oligomeric assemblies. *Journal of neuroscience research* **69**, 567–577 (2002).
42. Haass, C. & Selkoe, D. J. Soluble protein oligomers in neurodegeneration: lessons from the Alzheimer’s amyloid β -peptide. *Nature reviews Molecular cell biology* **8**, 101–112 (2007).
43. Kaye, R. & Lasagna-Reeves, C. A. Molecular mechanisms of amyloid oligomers toxicity. *Journal of Alzheimer’s Disease* **33**, S67–S78 (2013).

44. Citron, M. *et al.* Mutation of the β -amyloid precursor protein in familial Alzheimer's disease increases β -protein production. *Nature* **360**, 672–674 (1992).
45. Nilsberth, C. *et al.* The 'Arctic' APP mutation (E693G) causes Alzheimer's disease by enhanced A β protofibril formation. *Nature neuroscience* **4**, 887–893 (2001).
46. Castellano, J. M. *et al.* Human apoE isoforms differentially regulate brain amyloid- β peptide clearance. *Science translational medicine* **3**, 89ra57 (2011).
47. Jin, M. *et al.* Soluble amyloid β -protein dimers isolated from Alzheimer cortex directly induce Tau hyperphosphorylation and neuritic degeneration. *Proceedings of the National Academy of Sciences* **108**, 5819–5824 (2011).
48. Song, M., Rauw, G., Baker, G. & Kar, S. Memantine protects rat cortical cultured neurons against β -amyloid-induced toxicity by attenuating tau phosphorylation. *European Journal of Neuroscience* **28**, 1989–2002 (2008).
49. Shankar, G. M. *et al.* Amyloid- β protein dimers isolated directly from Alzheimer's brains impair synaptic plasticity and memory. *Nature medicine* **14**, 837–842 (2008).
50. Sperling, R. A. *et al.* Toward defining the preclinical stages of Alzheimer's disease: recommendations from the National Institute on Aging-Alzheimer's Association workgroups on diagnostic guidelines for Alzheimer's disease. *Alzheimer's & Dementia: The Journal of the Alzheimer's Association* **7**, 280–292 (2011).
51. Panza, F., Loupone, M., Logroscino, G. & Imbimbo, B. P. A critical appraisal of amyloid- β -targeting therapies for Alzheimer disease. *Nature Reviews Neurology* **15**, 73–88 (2019).
52. Herrup, K. The case for rejecting the amyloid cascade hypothesis. *Nature neuroscience* **18**, 794–799 (2015).
53. Howard, R. & Liu, K. Y. Questions EMERGE as Biogen claims aducanumab turnaround. *Nature Reviews Neurology* **16**, 63–64 (2020).
54. Knopman, D. S., Jones, D. T. & Greicius, M. D. Failure to demonstrate efficacy of aducanumab: An analysis of the EMERGE and ENGAGE trials as reported by Biogen, December 2019. *Alzheimer's & Dementia: The Journal of the Alzheimer's Association* **17**, 696–701 (2020).
55. Kolarova, M., García-Sierra, F., Bartos, A., Ricny, J. & Ripova, D. Structure and pathology of tau protein in Alzheimer disease. *International journal of Alzheimer's disease* **2012** (2012).
56. Shamma, S. L. *et al.* A mechanistic model of tau amyloid aggregation based on direct observation of oligomers. *Nature communications* **6**, 1–10 (2015).
57. Alonso, A. d. C., Zaidi, T., Grundke-Iqbal, I. & Iqbal, K. Role of abnormally phosphorylated tau in the breakdown of microtubules in Alzheimer disease. *Proceedings of the National Academy of Sciences* **91**, 5562–5566 (1994).

58. Wu, J. W. *et al.* Neuronal activity enhances tau propagation and tau pathology in vivo. *Nature neuroscience* **19**, 1085–1092 (2016).
59. Bachurin, S. O., Bovina, E. V. & Ustyugov, A. A. Drugs in clinical trials for Alzheimer's disease: the major trends. *Medicinal research reviews* **37**, 1186–1225 (2017).
60. Martin, L. *et al.* Tau protein kinases: involvement in Alzheimer's disease. *Ageing research reviews* **12**, 289–309 (2013).
61. Engel, T., Goñi-Oliver, P., Lucas, J. J., Avila, J. & Hernández, F. Chronic lithium administration to FTDP-17 tau and GSK-3 β overexpressing mice prevents tau hyperphosphorylation and neurofibrillary tangle formation, but pre-formed neurofibrillary tangles do not revert. *Journal of neurochemistry* **99**, 1445–1455 (2006).
62. De Barreda, E. G. *et al.* Tau-knockout mice show reduced GSK3-induced hippocampal degeneration and learning deficits. *Neurobiology of disease* **37**, 622–629 (2010).
63. Hoshi, M. *et al.* Regulation of mitochondrial pyruvate dehydrogenase activity by tau protein kinase I/glycogen synthase kinase 3 β in brain. *Proceedings of the National Academy of Sciences* **93**, 2719–2723 (1996).
64. Lovestone, S. *et al.* A phase II trial of tideglusib in Alzheimer's disease. *Journal of Alzheimer's Disease* **45**, 75–88 (2015).
65. Congdon, E. E. & Sigurdsson, E. M. Tau-targeting therapies for Alzheimer disease. *Nature Reviews Neurology* **14**, 399–415 (2018).
66. Martin, L. *et al.* Tau protein phosphatases in Alzheimer's disease: the leading role of PP2A. *Ageing research reviews* **12**, 39–49 (2013).
67. Tanimukai, H., Grundke-Iqbal, I. & Iqbal, K. Up-regulation of inhibitors of protein phosphatase-2A in Alzheimer's disease. *The American journal of pathology* **166**, 1761–1771 (2005).
68. Yao, X.-Q. *et al.* Glycogen synthase kinase-3 β regulates Tyr307 phosphorylation of protein phosphatase-2A via protein tyrosine phosphatase 1B but not Src. *Biochemical Journal* **437**, 335–344 (2011).
69. Yiannopoulou, K. G. & Papageorgiou, S. G. Current and future treatments in Alzheimer disease: an update. *Journal of central nervous system disease* **12**, 1–12 (2020).
70. Cascella, R. & Cecchi, C. Calcium Dyshomeostasis in Alzheimer's Disease Pathogenesis. *International Journal of Molecular Sciences* **22**, 4914 (2021).
71. Clapham, D. E. Calcium signaling. *Cell* **131**, 1047–1058 (2007).
72. O'Day, D. H. & Myre, M. A. Calmodulin-binding domains in Alzheimer's disease proteins: extending the calcium hypothesis. *Biochemical and biophysical research communications* **320**, 1051–1054 (2004).

73. Reese, L. C. & Tagliatela, G. A role for calcineurin in Alzheimer's disease. *Current neuropharmacology* **9**, 685–692 (2011).
74. Danysz, W. & Parsons, C. G. The NMDA receptor antagonist memantine as a symptomatological and neuroprotective treatment for Alzheimer's disease: preclinical evidence. *International journal of geriatric psychiatry* **18**, S23–S32 (2003).
75. Liu, J., Chang, L., Song, Y., Li, H. & Wu, Y. The role of NMDA receptors in Alzheimer's disease. *Frontiers in neuroscience* **13**, 1–43 (2019).
76. Massey, P. V. *et al.* Differential roles of NR2A and NR2B-containing NMDA receptors in cortical long-term potentiation and long-term depression. *Journal of Neuroscience* **24**, 7821–7828 (2004).
77. Palop, J. J. & Mucke, L. Amyloid- β -induced neuronal dysfunction in Alzheimer's disease: from synapses toward neural networks. *Nature neuroscience* **13**, 812–818 (2010).
78. Wang, Z.-C., Zhao, J. & Li, S. Dysregulation of synaptic and extrasynaptic N-methyl-D-aspartate receptors induced by amyloid- β . *Neuroscience bulletin* **29**, 752–760 (2013).
79. Chavez, S. E. & O'Day, D. H. Calmodulin binds to and regulates the activity of beta-secretase (BACE1). *Curr Res Alzheimers Dis* **1**, 37–47 (2007).
80. Padilla, R., Maccioni, R. B. & Avila, J. Calmodulin binds to a tubulin binding site of the microtubule-associated protein tau. *Molecular and cellular biochemistry* **97**, 35–41 (1990).
81. Baudier, J. *et al.* Comparison of S100b protein with calmodulin: Interactions with melittin and microtubule-associated τ proteins and inhibition of phosphorylation of τ proteins by protein kinase C. *Biochemistry* **26**, 2886–2893 (1987).
82. Wu, H.-Y. *et al.* Amyloid β induces the morphological neurodegenerative triad of spine loss, dendritic simplification, and neuritic dystrophies through calcineurin activation. *Journal of Neuroscience* **30**, 2636–2649 (2010).
83. Mansuy, I. M. Calcineurin in memory and bidirectional plasticity. *Biochemical and biophysical research communications* **311**, 1195–1208 (2003).
84. Rozkalne, A., Hyman, B. T. & Spires-Jones, T. L. Calcineurin inhibition with FK506 ameliorates dendritic spine density deficits in plaque-bearing Alzheimer model mice. *Neurobiology of disease* **41**, 650–654 (2011).
85. O'Day, D. H., Eshak, K. & Myre, M. A. Calmodulin binding proteins and Alzheimer's disease. *Journal of Alzheimer's Disease* **46**, 553–569 (2015).
86. Yin, Y. *et al.* Tau accumulation induces synaptic impairment and memory deficit by calcineurin-mediated inactivation of nuclear CaMKIV/CREB signaling. *Proceedings of the National Academy of Sciences* **113**, 3773–3781 (2016).

87. Sakagami, H. *et al.* Prominent expression and activity-dependent nuclear translocation of Ca²⁺/calmodulin-dependent protein kinase I δ in hippocampal neurons. *European Journal of Neuroscience* **22**, 2697–2707 (2005).
88. Johannessen, M., Delghandi, M. P. & Moens, U. What turns CREB on? *Cellular signalling* **16**, 1211–1227 (2004).
89. Hardingham, G. E., Fukunaga, Y. & Bading, H. Extrasynaptic NMDARs oppose synaptic NMDARs by triggering CREB shut-off and cell death pathways. *Nature neuroscience* **5**, 405–414 (2002).
90. Yamamoto-Sasaki, M., Ozawa, H., Saito, T., Rösler, M. & Riederer, P. Impaired phosphorylation of cyclic AMP response element binding protein in the hippocampus of dementia of the Alzheimer type. *Brain research* **824**, 300–303 (1999).
91. Bartolotti, N., Bennett, D. & Lazarov, O. Reduced pCREB in Alzheimer’s disease prefrontal cortex is reflected in peripheral blood mononuclear cells. *Molecular psychiatry* **21**, 1158–1166 (2016).
92. Pugazhenti, S., Wang, M., Pham, S., Sze, C.-I. & Eckman, C. B. Downregulation of CREB expression in Alzheimer’s brain and in A β -treated rat hippocampal neurons. *Molecular neurodegeneration* **6**, 1–16 (2011).
93. Müller, M., Cárdenas, C., Mei, L., Cheung, K.-H. & Foskett, J. K. Constitutive cAMP response element binding protein (CREB) activation by Alzheimer’s disease presenilin-driven inositol trisphosphate receptor (InsP₃R) Ca²⁺ signaling. *Proceedings of the National Academy of Sciences* **108**, 13293–13298 (2011).
94. Satoh, J.-i., Tabunoki, H. & Arima, K. Molecular network analysis suggests aberrant CREB-mediated gene regulation in the Alzheimer disease hippocampus. *Disease markers* **27**, 239–252 (2009).
95. Papadia, S., Stevenson, P., Hardingham, N. R., Bading, H. & Hardingham, G. E. Nuclear Ca²⁺ and the cAMP response element-binding protein family mediate a late phase of activity-dependent neuroprotection. *Journal of Neuroscience* **25**, 4279–4287 (2005).
96. Amritraj, A. *et al.* Role of cathepsin D in U18666A-induced neuronal cell death: potential implication in Niemann-Pick type C disease pathogenesis. *Journal of Biological Chemistry* **288**, 3136–3152 (2013).
97. Takashima, A. *et al.* Exposure of rat hippocampal neurons to amyloid β peptide (25–35) induces the inactivation of phosphatidylinositol-3 kinase and the activation of tau protein kinase I/glycogen synthase kinase-3 β . *Neuroscience letters* **203**, 33–36 (1996).
98. Bright, J. *et al.* Human secreted tau increases amyloid-beta production. *Neurobiology of aging* **36**, 693–709 (2015).

99. Ho, R., Ortiz, D. & Shea, T. B. Amyloid- β promotes calcium influx and neurodegeneration via stimulation of L voltage-sensitive calcium channels rather than NMDA channels in cultured neurons. *Journal of Alzheimer's Disease* **3**, 479–483 (2001).
100. Yoshimura, Y., Ichinose, T. & Yamauchi, T. Phosphorylation of tau protein to sites found in Alzheimer's disease brain is catalyzed by Ca^{2+} /calmodulin-dependent protein kinase II as demonstrated tandem mass spectrometry. *Neuroscience Letters* **353**, 185–188 (2003).
101. Mahoney, R. *et al.* Pathogenic Tau causes a toxic depletion of nuclear calcium. *Cell reports* **32**, 107900 (2020).
102. Ghosh, A. & Giese, K. P. Calcium/calmodulin-dependent kinase II and Alzheimer's disease. *Molecular brain* **8**, 1–7 (2015).
103. Yamagata, Y. *et al.* Kinase-dead knock-in mouse reveals an essential role of kinase activity of Ca^{2+} /calmodulin-dependent protein kinase II α in dendritic spine enlargement, long-term potentiation, and learning. *Journal of Neuroscience* **29**, 7607–7618 (2009).
104. Borgesius, N. Z. *et al.* β CaMKII plays a nonenzymatic role in hippocampal synaptic plasticity and learning by targeting α CaMKII to synapses. *Journal of Neuroscience* **31**, 10141–10148 (2011).
105. Fink, C. C. *et al.* Selective regulation of neurite extension and synapse formation by the β but not the α isoform of CaMKII. *Neuron* **39**, 283–297 (2003).
106. Lee, S.-J. R., Escobedo-Lozoya, Y., Szatmari, E. M. & Yasuda, R. Activation of CaMKII in single dendritic spines during long-term potentiation. *Nature* **458**, 299–304 (2009).
107. Matthews, R. P. *et al.* Calcium/calmodulin-dependent protein kinase types II and IV differentially regulate CREB-dependent gene expression. *Molecular and cellular biology* **14**, 6107–6116 (1994).
108. Reese, L. C., Laezza, F., Woltjer, R. & Tagliatela, G. Dysregulated phosphorylation of Ca^{2+} /calmodulin-dependent protein kinase II- α in the hippocampus of subjects with mild cognitive impairment and Alzheimer's disease. *Journal of neurochemistry* **119**, 791–804 (2011).
109. Gu, Z., Liu, W. & Yan, Z. β -Amyloid impairs AMPA receptor trafficking and function by reducing Ca^{2+} /calmodulin-dependent protein kinase II synaptic distribution. *Journal of Biological Chemistry* **284**, 10639–10649 (2009).
110. Jiang, X. *et al.* Spatial training preserves associative memory capacity with augmentation of dendrite ramification and spine generation in Tg2576 mice. *Scientific reports* **5**, 1–8 (2015).
111. Ashpole, N. M. *et al.* Calcium/calmodulin-dependent protein kinase II (CaMKII) inhibition induces neurotoxicity via dysregulation of glutamate/calcium signaling and hyperexcitability. *Journal of Biological Chemistry* **287**, 8495–8506 (2012).

112. Mairet-Coello, G. *et al.* The CAMKK2-AMPK Kinase Pathway Mediates the Synaptotoxic Effects of A β Oligomers through Tau Phosphorylation. *Neuron* **78**, 94–108 (2013).
113. Ishikawa, Y. *et al.* Identification and characterization of novel components of a Ca²⁺/calmodulin-dependent protein kinase cascade in HeLa cells. *FEBS letters* **550**, 57–63 (2003).
114. Thornton, C., Bright, N. J., Sastre, M., Muckett, P. J. & Carling, D. AMP-activated protein kinase (AMPK) is a tau kinase, activated in response to amyloid β -peptide exposure. *Biochemical Journal* **434**, 503–512 (2011).
115. Chang, F., Zhang, L.-H., Xu, W.-P., Jing, P. & Zhan, P.-Y. microRNA-9 attenuates amyloid β -induced synaptotoxicity by targeting calcium/calmodulin-dependent protein kinase kinase 2. *Molecular Medicine Reports* **9**, 1917–1922 (2014).
116. Lee, A. *et al.* A β 42 oligomers trigger synaptic loss through CAMKK2-AMPK-dependent effectors coordinating mitochondrial fission and mitophagy. *bioRxiv preprint*, 1–26 (2019).
117. Sabbir, M. G. Loss of Ca²⁺/Calmodulin Dependent Protein Kinase Kinase 2 Leads to Aberrant Transferrin Phosphorylation and Trafficking: A Potential Biomarker for Alzheimer's Disease. *Frontiers in Molecular Biosciences* **5**, 1–28 (2018).
118. Fukushima, H. *et al.* Upregulation of Calcium/Calmodulin-Dependent Protein Kinase IV Improves Memory Formation and Rescues Memory Loss with Aging. *The Journal of Neuroscience* **28**, 9910–9919 (2008).
119. Anderson, K. A., Noeldner, P. K., Reece, K., Wadzinski, B. E. & Means, A. R. Regulation and function of the calcium/calmodulin-dependent protein kinase IV/protein serine/threonine phosphatase 2A signaling complex. *Journal of Biological Chemistry* **279**, 31708–31716 (2004).
120. Ye, T. *et al.* Chrysophanol improves memory ability of d-galactose and A β 25-35 treated rat correlating with inhibiting tau hyperphosphorylation and the CaM–CaMKIV signal pathway in hippocampus. *3 Biotech* **10**, 111 (2020).
121. Akizuki, K. *et al.* Biochemical characterization of four splice variants of mouse Ca²⁺/calmodulin-dependent protein kinase I δ . *The Journal of Biochemistry* **169**, 445–458 (2021).
122. Verploegen, S., Lammers, J.-W. J., Koenderman, L. & Coffey, P. J. Identification and characterization of CKLiK, a novel granulocyte Ca⁺⁺/calmodulin-dependent kinase. *Blood* **96**, 3215–3223 (2000).
123. Kamata, A. *et al.* Spatiotemporal expression of four isoforms of Ca²⁺/calmodulin-dependent protein kinase I in brain and its possible roles in hippocampal dendritic growth. *Neuroscience research* **57**, 86–97 (2007).
124. Liang, X. *et al.* Genomic convergence to identify candidate genes for Alzheimer disease on chromosome 10. *Human mutation* **30**, 463–471 (2009).

125. Floudas, C. S., Um, N., Kamboh, M. I., Barmada, M. M. & Visweswaran, S. Identifying genetic interactions associated with late-onset Alzheimer's disease. *BioData mining* **7**, 35 (2014).
126. Zhao, J. *et al.* A genome-wide profiling of brain DNA hydroxymethylation in Alzheimer's disease. *Alzheimer's & Dementia: The Journal of the Alzheimer's Association* **13**, 674–688 (2017).
127. Bernstein, A. I. *et al.* 5-Hydroxymethylation-associated epigenetic modifiers of Alzheimer's disease modulate Tau-induced neurotoxicity. *Human Molecular Genetics* **25**, 2437–2450 (2016).
128. Xu, S. *et al.* 5-Hydroxymethylcytosine Signatures in Circulating Cell-Free DNA as Diagnostic Biomarkers for Late-Onset Alzheimer's Disease. *Preprints with The Lancet*, 1–32 (2021).
129. Riascos, D. *et al.* Alterations of Ca²⁺-responsive proteins within cholinergic neurons in aging and Alzheimer's disease. *Neurobiology of Aging* **35**, 1325–1333 (2014).
130. Bergamaschi, A. *et al.* CAMK1D amplification implicated in epithelial–mesenchymal transition in basal-like breast cancer. *Molecular oncology* **2**, 327–339 (2008).
131. Curtis, C. *et al.* The genomic and transcriptomic architecture of 2,000 breast tumours reveals novel subgroups. *Nature* **486**, 346–352 (2012).
132. Zeggini, E. *et al.* Meta-analysis of genome-wide association data and large-scale replication identifies additional susceptibility loci for type 2 diabetes. *Nature genetics* **40**, 638–645 (2008).
133. Shu, X. O. *et al.* Identification of new genetic risk variants for type 2 diabetes. *PLoS genetics* **6**, e1001127 (2010).
134. Kooner, J. S. *et al.* Genome-wide association study in individuals of South Asian ancestry identifies six new type 2 diabetes susceptibility loci. *Nature genetics* **43**, 984–989 (2011).
135. Morris, A. P. *et al.* Large-scale association analysis provides insights into the genetic architecture and pathophysiology of type 2 diabetes. *Nature genetics* **44**, 981 (2012).
136. Haney, S. *et al.* RNAi screening in primary human hepatocytes of genes implicated in genome-wide association studies for roles in type 2 diabetes identifies roles for CAMK1D and CDKAL1, among others, in hepatic glucose regulation. *PloS one* **8**, e64946 (2013).
137. Fromont, C. *et al.* Discovery of Highly Selective Inhibitors of Calmodulin-Dependent Kinases That Restore Insulin Sensitivity in the Diet-Induced Obesity in Vivo Mouse Model. *Journal of Medicinal Chemistry* **63**, 6784–6801 (2020).

138. Yin, L., Duan, J.-J., Bian, X.-W. & Yu, S.-c. Triple-negative breast cancer molecular subtyping and treatment progress. *Breast Cancer Research* **22**, 1–13 (2020).
139. Loo, L. W. *et al.* Genome-wide copy number alterations in subtypes of invasive breast cancers in young white and African American women. *Breast cancer research and treatment* **127**, 297–308 (2011).
140. Yamada, T. *et al.* Effects of PU. 1-induced mouse calcium–calmodulin-dependent kinase I-like kinase (CKLiK) on apoptosis of murine erythroleukemia cells. *Experimental cell research* **294**, 39–50 (2004).
141. Smith, B. E. *et al.* Differential PROTAC substrate specificity dictated by orientation of recruited E3 ligase. *Nature communications* **10**, 1–13 (2019).
142. Sun, X. *et al.* PROTACs: great opportunities for academia and industry. *Signal transduction and targeted therapy* **4**, 1–33 (2019).
143. McLennan, S. *Structural & Kinetic Studies of CaMK1D Interactions* Master’s thesis (University of Alberta, Edmonton, AB, 2018).
144. Fa, M. *et al.* Preparation of oligomeric β -amyloid1-42 and induction of synaptic plasticity impairment on hippocampal slices. *Journal of visualized experiments: JoVE* (2010).
145. Cizas, P. *et al.* Size-dependent neurotoxicity of β -amyloid oligomers. *Archives of biochemistry and biophysics* **496**, 84–92 (2010).
146. Fairhead, M. & Howarth, M. in *Site-Specific Protein Labeling* 171–184 (Springer, 2015).
147. Yung-Chi, C. & Prusoff, W. H. Relationship between the inhibition constant (KI) and the concentration of inhibitor which causes 50 per cent inhibition (I50) of an enzymatic reaction. *Biochemical pharmacology* **22**, 3099–3108 (1973).
148. Hornbeck, P. *et al.* PhosphoSitePlus: mutations, PTMs and recalibrations. *Nucleic Acids Research* **43**, D512–20 (2014).
149. Takemoto-Kimura, S. *et al.* Molecular cloning and characterization of CLICK-III/CaMKI γ , a novel membrane-anchored neuronal Ca²⁺/calmodulin-dependent protein kinase (CaMK). *Journal of Biological Chemistry* **278**, 18597–18605 (2003).
150. Wayman, G. A. *et al.* Activity-dependent dendritic arborization mediated by CaM-kinase I activation and enhanced CREB-dependent transcription of Wnt-2. *Neuron* **50**, 897–909 (2006).
151. Suárez-Calvet, M. *et al.* Novel tau biomarkers phosphorylated at T181, T217 or T231 rise in the initial stages of the preclinical Alzheimer’s continuum when only subtle changes in A β pathology are detected. *EMBO Molecular Medicine* **12**, e12921 (2020).

152. Marambaud, P., Dreses-Werringloer, U. & Vingtdeux, V. Calcium signaling in neurodegeneration. *Molecular neurodegeneration* **4**, 1–15 (2009).
153. Bian, Y. *et al.* An enzyme assisted RP-RPLC approach for in-depth analysis of human liver phosphoproteome. *Journal of proteomics* **96**, 253–262 (2014).